Estimating the Spatiotemporal Variation of NO_2 Concentration Using Adaptive Neuro-Fuzzy Inference System

*Bijan Yeganeh[1, 2], Michael G. Hewson[3], Samuel Clifford[2, 4], Ahmad Tavassoli[5], Luke D. Knibbs[6], and Lidia Morawska[1, *]*

[1] International Laboratory for Air Quality and Health, Queensland University of Technology, Brisbane, Queensland 4001, Australia

[2] Centre for Air quality and health Research and evaluation, Glebe, New South Wales 2037, Australia

[3] School of Education and the Arts, Central Queensland University, North Rockhampton, Queensland 4702, Australia

[4] ARC Centre of Excellence for Mathematical and Statistical Frontiers, Queensland University of Technology, Brisbane, Queensland 4001, Australia

[5] School of Civil Engineering, The University of Queensland, St Lucia, Queensland 4072, Australia

[6] School of Public Health, The University of Queensland, Herston, Queensland 4006, Australia

*** Corresponding author:** Professor Lidia Morawska, PhD

International Laboratory for Air Quality and Health

Queensland University of Technology, Brisbane, Queensland 4001, Australia

Phone: +61 7 3138 2616

Fax: +61 7 3138 9079

Email: l.morawska@qut.edu.au

Abstract

Statistical modelling has been successfully used to estimate the variations of NO_2 concentration, but employing new modelling techniques can make these estimations far more accurate. To do so, for the first time in application to spatiotemporal air pollution modelling, we employed a soft computing algorithm called adaptive neuro-fuzzy inference system (ANFIS) to estimate the NO_2 variations. Comprehensive data sets were investigated to determine the most effective predictors for the modelling process, including land use, meteorological, satellite, and traffic variables. We have demonstrated that using selected satellite, traffic, meteorological, and land use predictors in modelling increased the R^2 by 21%, and decreased the root mean square error (RMSE) by 47% compared with the model only trained by land use and meteorological predictors. The ANFIS model found to have better performance and higher accuracy than the multiple regression model. Our best model, captures 91% of the spatiotemporal variability of monthly mean NO_2 concentrations at 1 km spatial resolution (RMSE 1.49 ppb) in a selected area of Australia.

Keywords: NO_2; Satellite data; ANFIS; Spatiotemporal; Transport model; Australia.

Data availability

The type and source of the data set considered in this study.

Name of the data set	Data source (Developer) (All websites accessed on April 2016)	Data format	Software required	Data availability
OMI tropospheric NO_2 column density (molecules × 10^{15}/cm^2)	Aura OMI tropospheric NO_2 column density product via NASA Giovanni interface http://giovanni.sci.gsfc.nasa.gov/giovanni/?instance_id=omil2g	HDF / NetCDF files	ArcGIS	Freely available
Major road	PSMA Australia Transport and Topography product https://www.psma.com.au/products/transport-topography	ESRI shape files	" "	Price depends on the area of interest
Minor road	" "	" "	" "	" "
Industrial point source NOx emissions	Australia National Pollutant Inventory http://www.npi.gov.au/reporting/industry-reporting-materials	xml files	Microsoft Excel / R	Freely available
Australia population density	Australian Bureau of Statistics http://www.abs.gov.au/ausstats/abs@.nsf/mf/1270.0.55.007	PNG ESRI Grid GeoTIFF	ArcGIS	" "
Australia land use classification	Australian Bureau of Statistics http://www.abs.gov.au/websitedbs/censushome.nsf/home/meshblockcounts	Excel spreadsheets / CSV files	Microsoft Excel / R / ArcGIS	" "
Elevation	U.S. Geological Survey https://www.usgs.gov/products/maps/topo-maps	PNG GeoTIFF	ArcGIS	" "
Normalized difference vegetation index	Terrestrial Ecosystem Research Network http://www.auscover.org.au/node/9	NetCDF files	" "	" "
Temperature Rainfall Humidity Solar exposure	Australian Bureau of Meteorology http://www.bom.gov.au/climate/maps/#tabs=Maps	ESRI Grid GIF	" "	" "
Traffic data	Department of Transport and Main Roads http://www.tmr.qld.gov.au/Travel-and-transport/Road-and-traffic-info/Traffic-reports-and-road-conditions	ESRI shape files	" "	Price depends on the area of interest

Software availability

The following software has been used in this study for statistical analysis, spatial data processing, map creation, and calculating the meteorological and traffic-related parameters:

- R v. 3.2.3 (R Foundation for Statistical Computing, Vienna, Austria)
- MATLAB R2014b (MathWorks Inc., Natick, USA)
- ArcGIS v.10.2 (ESRI Inc., Redlands, USA)
- Weather Research and Forecasting v 3.8.1 (Powers et al., 2008)
- South-east Queensland Strategic Transport Model (Ryan et al., 2008)

Note: No specific software component has been developed for this study.

1. Introduction

Exposure to ambient air pollution is a major environmental risk factor associated with adverse health effects (Forouzanfar et al., 2015). Nitrogen dioxide (NO_2) is a major component of ambient air pollution and a strong marker of traffic-related emissions (Briggs et al., 1997; Richter et al., 2005). To date, epidemiological studies have demonstrated that there are adverse health effects associated with exposure to NO_2 (Crouse et al., 2010; Crouse et al., 2015; Filleul et al., 2005; Mölter et al., 2014; Parent et al., 2013; Perez et al., 2012). In addition, NO_2 is recognized as a good proxy of particle number concentration in urban environments (Grundström et al., 2015). Hence more precise estimates of NO_2 concentration is needed to investigate its associated role on health effects.

Fossil fuel combustion including coal, gas and oil, are the major sources of NO_2 in Australia (Australian Government, 2010). As a subset of this, traffic related emissions are a major source of NO_2 in urban areas (Derwent and Hertel, 1998). About 80% of the NO_2 in Australian urban areas comes from motor vehicle exhaust (Australian Government, 2010). This indicates that traffic flow needs to be carefully investigated for estimating the NO_2 concentration in Australia as one of the most urbanized countries in the world.

Different approaches have been used to provide a proxy for traffic flow including calculating the length of the roads or road classification (Henderson et al., 2007; Knibbs et al., 2014; Sahsuvaroglu et al., 2006), and using nearest traffic count (Dirgawati et al., 2015; Ducret-Stich et al., 2013). Some studies used transportation models to obtain more accurate estimates of traffic flow, and this approach has been found to provide better results than previous approaches (Costabile and Allegrini, 2008; Kim and Guldmann, 2011, 2015; Shekarrizfard et al., 2015).

Moreover, traffic dynamics can also significantly affect the NO_2 emissions, as congested traffic (e.g. stop-and-go traffic) results in particulate matters and gaseous emissions peak beyond the free-flow traffic condition (Davis and Peckham, 2007; Giakoumis et al., 2012; Hagena et al., 2006; Keuken et al., 2010; Rakopoulos and Giakoumis, 2009). Consequently, traffic dynamics and condition plays a significant role in the emission of NO_2 from vehicles in urban areas and should be investigated during the NO_2 modelling process.

Estimates of air pollution concentration have been traditionally provided by ground monitoring networks. The sparse ground measurement network in many parts of the world, including Australia makes it difficult to evaluate the spatiotemporal variability of ambient air pollution. Even a dense network could not adequately monitor the spatiotemporal variability of ambient air pollution, since it is changing on scales much smaller than monitoring networks density. This represents a significant limitation on evaluating the adverse health effects associated with ambient air pollution.

Satellite imagery is another important tool rapidly gaining interest in air pollution monitoring as it provides sequential observations with extensive spatial coverage (Kloog et al., 2014). Data derived from satellite sensors can be combined with ground-based measurements at different spatiotemporal scales (Reis et al., 2015). The availability of satellite-derived data has helped to overcome the problems associated with sparse monitoring networks by providing observations where previously there were none (Martin, 2008; Reis et al., 2015).

Observation-based statistical methods have emerged as a powerful tool for exploring the quantitative relationship between ground-level NO_2 concentrations and satellite-derived data, and a variety of these methods have been used to quantify this relationship (Bechle et al., 2015; Carnevale et al., 2016; Hoek et al., 2015; Horsburgh et al., 2016; Hystad et al., 2011; Knibbs et al., 2014; Novotny et al., 2011; Reggente et al., 2014; Vienneau et al., 2013). Machine

learning refers to computational techniques which are able to achieve optimal solutions for analyzing complicated phenomena at reasonable costs (Kruse et al., 2013; Ovaska, 2004). In recent years, machine learning algorithms including support vector machine (SVM) (Moazami et al., 2016; Reid et al., 2015; Yeganeh et al., 2012), Bayesian models (Corani and Scanagatta, 2016; McBride et al., 2007), *k*-nearest neighbours (kNN) (Reid et al., 2015), and artificial neural network (ANN) (Agirre-Basurko et al., 2006; Al-Alawi et al., 2008; Ordieres et al., 2005; Wu et al., 2012; Yeganeh et al., 2017) have also been gaining popularity because of their high flexibility and proven prediction abilities. The literature however, indicates that adaptive neuro-fuzzy inference system (ANFIS), which is accepted as a robust and effective method for multivariate analysis, has not been used to date to estimate the spatiotemporal variation of NO_2 concentrations using satellite-based data.

While some studies have been conducted to investigate the spatial variation of the NO_2 in Australia (Dirgawati et al., 2015; Knibbs et al., 2014), recent studies have shown that the combination of temporal variables (e.g. satellite-based observations and metrological data) with temporally fixed geographical factors can improve the predictive ability and extend the temporal coverage of the statistical models applied for quantifying the ambient air pollution (Bechle et al., 2015; Eeftens et al., 2011; Gulliver et al., 2013; Mölter et al., 2010; Rose et al., 2011; Sampson et al., 2011). Therefore, there is a clear need to develop a spatiotemporal NO_2 model accounting for both spatial and spatiotemporal variables, in the context of Australia.

In this study, we aimed to significantly enhance the spatiotemporal estimates of NO_2 concentration by using satellite-based and traffic data in conjunction with comprehensive meteorological and geographical data. Further, for the first time, we used a transport model to estimate the volume of traffic flow and traffic dynamics (congestion) for all of the individual roads and employed them for estimating NO_2 concentration. Adaptive neuro-fuzzy inference system (ANFIS) was employed to estimate the monthly average concentration of NO_2 in a

selected area of Australia, from 2006 to 2011, and to calculate population-weighted NO_2 concentration in urban areas located in the study area . In turn, a cross-validation technique was used for model validation.

2. Materials and Methods

2.1. Data collection

2.1.1. Study location and ground-level NO_2 measurements

This study was carried out in South-east Queensland (SEQ) which is located in the state of Queensland, Australia. SEQ has an area of 22,420 km^2, and it is home to 3.05 million people based on the 2011 Australian census (Australian Bureau of Statistics., 2012). The study area consists of Brisbane, the state's capital city, as well as other urban and rural centres including Ipswich, Logan City, Gold Coast, Sunshine Coast, and the Lockyer Valley.

Fossil fuels combustion such as oil, coal, and gas is the main source of NO_2 in Australia. Motor vehicle exhaust has the highest contribution to NO_2 emission in the Australian urban areas (Australian Government, 2010). Hourly NO_2 concentration is routinely measured by the Queensland government and other organizations in charge of regulatory ambient air pollution monitoring. Standard chemiluminescence method was used to measure NO_2 concentrations in SEQ monitoring network. We used quality-assured hourly NO_2 measurements from January 2006 to December 2011 at 12 monitoring sites across SEQ to obtain monthly averages of the NO_2 concentration. The location and the distance between the air quality monitoring stations are provided in supplements.

2.1.2. Satellite data

Daily measurements of NO_2 tropospheric column abundance were derived from the Ozone Monitoring Instrument (OMI) aboard the Aura satellite at a spatial resolution of 13 km × 24 km. OMI detects ultraviolet and visible solar backscatter radiation with a wide-field telescope using hyperspectral imaging, which provides almost worldwide coverage each day (NASA, 2007). Differential optical absorption spectroscopy (DOAS) retrieval method was employed to obtain the NO_2 tropospheric column density from OMI data (Levelt et al., 2006). Aura crosses the equator in a sun-synchronous polar orbit for the daylight ascending orbit (Torres et al., 2007), and passes over SEQ at approximately 14:00 local time. We chose the OMNO2d.v003 data set derived from OMI which is capable of providing near global, daily, 30% cloud screened, tropospheric, 0.25^0 spatial resolution, NO_2 column density. The monthly data sets were used to account for the sub-tropical location of the SEQ, where seasonal maritime air mass advection combined with topography often creates cloud cover during a large proportion of the Austral summer. We obtained the monthly average tropospheric NO_2 column density over SEQ from NASA Giovanni interface for each month from 2006–2011.

Normalized difference vegetation index (NDVI) was used to provide a measure of greenness and vegetation density. NDVI was employed to examine the impact of vegetation cover on NO_2 concentration in this study. The monthly mean NDVI data were retrieved from an Advanced Very High Resolution Radiometer (AVHRR) sensor carried on the National Oceanic and Atmospheric Administration (NOAA) satellite and processed by the Australian Bureau of Meteorology (BoM) at a spatial resolution of 1 km (Bureau of Meteorology, 2015).

2.1.3. Meteorological data

Meteorological parameters including planetary boundary layer height (PBLH), wind direction (WD) and wind speed (WS) were carefully investigated in this study. These parameters were calculated at a spatial resolution of 3 km at 14:00 local time to match the over-

pass time of the Aura satellite using Weather Research and Forecasting model (WRF). Details on the WRF configuration are provided in the supplement (pages S3-S6).

Other surface meteorological parameters including mean maximum and minimum temperatures, rainfall, and humidity were also examined in this study. These parameters were obtained from "high-quality spatial climate data sets" developed by the Australian Bureau of Meteorology (BoM) which provides gridded climatological maps for each month of the year (Jones et al., 2009). In addition, monthly solar exposure maps are obtained from BoM for the study period (Weymouth and Le Marshall, 2001).

2.1.4. Land use data

We obtained information on anthropogenic and natural land use data (spatial variables) that were potential predictors of NO_2 concentration. These variables provided estimates of emissions from point sources, changing land cover conditions, and distance to emission sources (Table 1).

2.1.5. Traffic data

In this paper, we used a four-stage aggregate transport model, the South East Queensland Strategic Transport Model (SEQSTM) to simulate current and future transport network of the study area (Ryan et al., 2008). The modelled road network includes all freeways, highways, arterials, and a selection of collector roads. All public transport routes including three modes, namely: bus, rail and ferry are also included with the details of service frequencies. The SEQSTM is based on the detailed knowledge of the factors affecting transport behaviours such as future changes in population, car ownership, employment, growth in households, and changes in the road and public transport networks. This model is typically used to predict variations in travel patterns, network flows, transport mode used, increase in general travel

volume, and the routing of trips (Evans et al., 2007). SEQSTM is able to calculate the average daily traffic volume (TRFV) for each road in the road network. This information was used to provide accurate proxies of traffic and to evaluate the traffic effect on NO_2 concentration.

A number of studies highlighted the impact of traffic congestion as a traffic attribute on air pollution (Bureau of Transport and Regional Economics., 2007; Luk et al., 2009). Traffic congestion mainly falls into two types: recurrent and non-recurrent. Random events such as adverse weather and work zones are the main reasons of non-recurrent congestion as these events temporarily decrease the capacity of a road, hence the peak demands exceed the normal amount. (Hojati et al., 2014). Recurrent congestion, in contrast, is triggered by chronically surpassed road capacity, which is a predictable event and can be determined by using transport models. Volume to capacity (V/C) ratio is a common congestion performance metric which has been used in many studies (Lomax, 1997). The threshold of this measure to be considered congestion depends on the road types. As suggested by Klop et al. (2008), a V/C ratio equal or higher than 0.8 can be considered congested. SEQSTM is used to calculate the average daily congestion based on the V/C measure on each link to provide a measure of congestion and assess its effect on NO_2 concentration.

The independent variables summarised in Table 1, were examined to discover which ones improved the prediction of NO_2 in our modelling process.

Table 1. Independent variables included as potential predictors of NO_2

Variables (units)	Spatial resolution	Point or buffer[a]	Data source
OMI tropospheric NO_2 column density (molecules × 10^{15} / cm^2)	13 × 24 km^2	Point	Aura OMI product via NASA Giovanni interface
Distance to Coast (km)	-	" "	ArcGIS geoprocessing tools
Distance to port (km)	-	" "	" "
Distance to airport (km)	-	" "	" "
Distance to nearest major road	-	" "	" "
Distance to nearest minor road	-	" "	" "
Airport (present/not present)	-	Buffer	" "
Major road (km)	-	" "	PSMA Australia Transport and Topography product
Minor road (km)	-	" "	" "
Industrial point source NO_x emissions (kg/yr)	-	" "	Australia National Pollutant Inventory
Time (Julian month)	-	Point	ArcGIS geoprocessing tools
Population density (person/km^2)	1 × 1 km^2	" "	Australian Bureau of Statistics
Land use by type (km^2)[b]	Mesh block[c]	Buffer	" "
Elevation (m)	30 m	Point	U.S. Geological Survey
Normalized difference vegetation index	1 × 1 km^2	" "	Terrestrial Ecosystem Research Network Derived from NASA NOAA satellite
Mean daily maximum temperature (°C)	5 × 5 km^2	" "	Australian Bureau of Meteorology
Mean daily minimum temperature (°C)	5 × 5 km^2	" "	" "
Rainfall (mm)	5 × 5 km^2	" "	" "
Humidity (hPa)	5 × 5 km^2	" "	" "
Solar exposure (MJ/m^2)	6 × 6 km^2	" "	" "
Planetary boundary layer height (m)	3 × 3 km^2	" "	Derived from Weather Research and Forecasting model
U-component of wind speed (m/s)	3 × 3 km^2	" "	" "
V-component of wind speed (m/s)	3 × 3 km^2	" "	" "
Wind speed (m/s)	3 × 3 km^2	" "	" "
Wind direction (Degrees)	3 × 3 km^2	" "	" "
Traffic volume (Passenger car unit)	-	Buffer	Derived from SEQSTM
Traffic-length (Passenger car unit × m)	-	" "	" "
Congestion frequency (No.)	-	" "	" "

[a] 22 Circular buffers were generated with radii of 50 m, 100 m, 200 m, 300 m, 400 m, 500 m, 600 m, 700 m, 800 m, 900 m, 1000 m, 1200 m, 1500 m, 1800 m, 2000 m, 2500 m, 3000 m, 3500 m, 4000 m, 5000 m, 7500 m, and 10,000 m (Novotny et al., 2011).

[b] Four different land use classes were investigated including industrial, commercial, residential, and open space (which contains the agricultural land, parks, and water bodies (Rose et al., 2010)).

[c] Mesh Block is the smallest geographic unit defined by the Australian Statistical Geography Standard for which the Census data is available (Australian Bureau of Statistics, 2011), and can be variable in size.

2.2. Modelling approach

In this study, independent variables were examined either as point or buffer variables. Point variables were extracted at each monitoring site (e.g., NDVI, humidity, wind speed), while buffer variables were computed within all buffer sizes (e.g., traffic volume, land use type). Following similar studies (Knibbs et al., 2014; Novotny et al., 2011), 22 circular buffers were created around each monitoring site to obtain local and more remote sources of NO_2 (Table 1). In total, 262 independent variables were obtained including 20 point variables and 242 buffer variables (11 variables computed at 22 buffer sizes).

To include the traffic data, we used TRFV which represents the average daily traffic volume for a link in a road network per year. A GIS layer containing TRFV data derived from SEQSTM was used to calculate TRFV within the buffer. In order to evaluate the effect of the distance traveled by each vehicle, the TRFV of each road segment was multiplied by its length to calculate the amount of traffic-length interaction (TRFL) in that given buffer, using Eq. 1:

$$TRFL_i = \sum_{j=1}^{n} TRFV_j \times length_j \quad (1)$$

where i, and j indicate the buffer sizes, and number of roads within each buffer respectively.

We also used SEQSTM results to calculate the average daily congestion based on the V/C ratio on each link (V/C > 0.8). The total number of congested roads was then counted to provide the frequency of the congestion occurrence within a buffer (CONF).

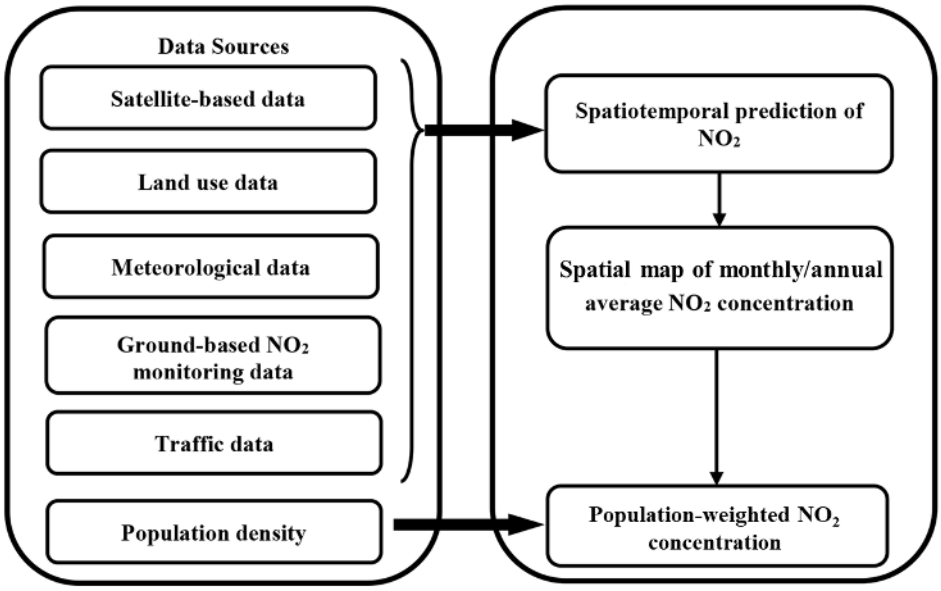

Figure 1. Conceptual approach for estimating population-weighted NO_2 concentration across SEQ.

2.3. Input selection

We followed "A Distance Decay Regression Selection Strategy" developed by Su et al. (2009) to select the best predictors for NO_2 models. In the following section, a brief description of this method is provided. For more detailed information see Su et al. (2009). As the first step, the correlations of the all independent variables with measured NO_2 were computed to obtain variable distance decay curves. The independent variable which had the highest correlation with the NO_2 measurements was selected as the first important predictor. A regression model was built by the first important predictor and NO_2 measurements. In the next step, the variable which had the highest correlation with the residuals of the regression model was chosen as the potential second important predictor, and the procedure replicated. To avoid multicollinearity, the new predictor was added to the model if the inclusion criteria were met. The criteria specified for this step were (a) the variance inflation factor (VIF) with parameters already in the regression model was less than 3, and (b) the significance level less than 0.05 (Su et al.,

2009). The process stopped when a new selected predictor failed to meet one of the inclusion criteria.

2.4. Adaptive neuro-fuzzy inference system (ANFIS)

ANFIS is a hybrid system that incorporates the strengths of fuzzy logic and artificial neural network (Jang, 1993; Lin and Lee, 1991). ANFIS combines the fuzzy principles with neural network learning abilities which provide an efficient technique for modelling.

Similar to multi-layer neural network, ANFIS consists of 5 layers. A fuzzy inference system is constructed in the first layer to extract a set of rules. In the following 4 layers, the adaptive learning algorithm is used to optimize the resulting parameters (Amini et al., 2008).

In the first layer (known as a fuzzifier), a fuzzy inference system (FIS) needs to be created in order to construct membership functions (MF) and extract the if-then rules for the input variables (Amini et al., 2008; Jang, 1993). In this study, Sugeno-type fuzzy inference system with Gaussian membership function is used, which has the following form:

$$MF_{ij} = exp\left[-\left(\frac{x-\bar{x}}{\sqrt{2}\delta}\right)^2\right] \quad \text{for} \quad i = 1, \dots, n \quad j = 1, \dots, m \tag{2}$$

where j shows the number of membership function associated with independent variable i, and δ and $\bar{x}$ indicate the variance and the mean of the Gaussian membership function (Jang, 1993). These functions minimize the number of rules by using "subtractive clustering" method and provide an effective model of the data behaviour (for more details see Jang and Gulley (1995)).

As the fuzzy logic is not able to learn from the input data (Mathur et al., 2016; Naji et al., 2016), a combination of the back-propagation gradient descent and least-squares learning procedures was utilized to provide ANFIS with adaptive learning abilities. (Jang, 1991, 1993; The Mathworks Inc., 2005). This adaptive learning process consists of 4 main steps. In the first step, the "product" operator is used to calculate the firing strength of the fuzzy rule (*w*) based

on the membership grade (μ) resulting from membership function. In the second step, the normalized firing strength ($\overline{w}$) for each rule is calculated (Amini et al., 2008). In the third step, an individual function is created for each variable using the consequent parameters derived from fuzzy rules (*f*) and its normalized firing strength (Mathur et al., 2016). Lastly, the sum of all the outputs resulting from the previous step is calculated to provide the final ANFIS outputs (Amini et al., 2008). Figure 2 shows the structure of ANFIS model used in this study.

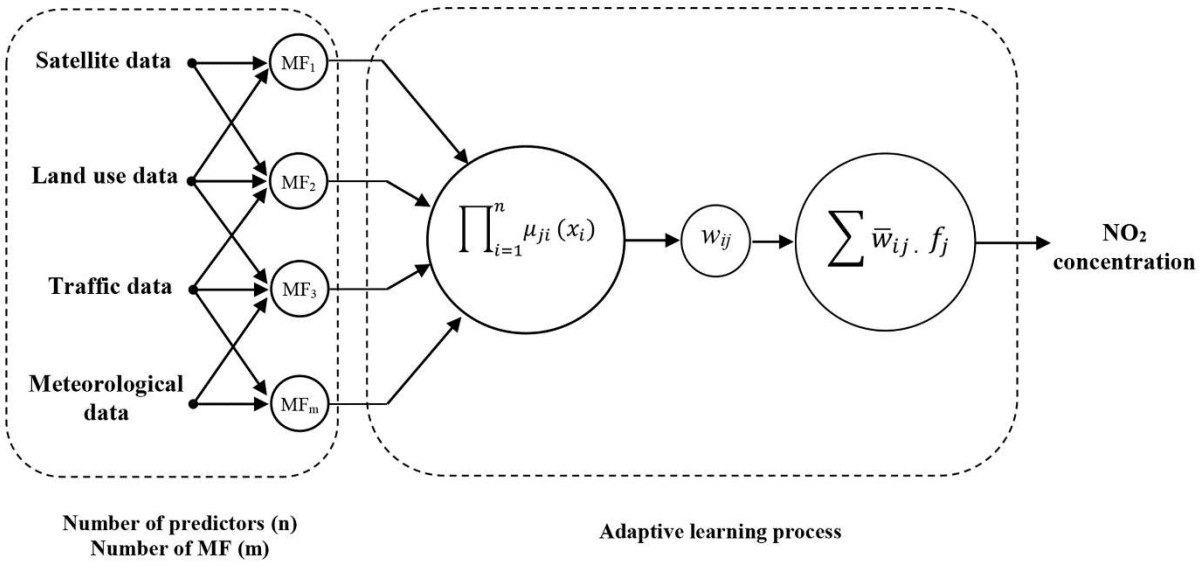

Figure 2. Schematic representation of ANFIS used to estimate NO_2 concentration.

As described in Section 2.3, "A Distance Decay Regression Selection Strategy" was employed to select the input data (predictors) for ANFIS model. The selected predictors were composed of different types of data, including meteorological, traffic, land use, and satellite data. These predictors were matched with the NO_2 concentration aligning measurement timings at 12 monitoring sites during the study period (72 months) which resulted in more than 800 observation sets in total. These observations were divided into training, validation, and test subsets. The majority of the observations (70%) were used for training the ANFIS model. Training dataset was used to adjust the model weights and derive the required coefficients. In order to avoid overfitting, 15% of the observations were used for internal validation process and checking the model's generalization (Wu et al., 2012). This dataset was employed to

minimize overfitting which means ANFIS verified that any increase in accuracy over the training dataset resulted in a rise in accuracy over an out of sample dataset that has not been shown to the model before. Finally, the remaining 15% of the observations were employed as the test subset to estimate the NO_2 concentration by the models. At this stage, the predictive ability of the ANFIS model was tested against the measurements, and the R^2 value was also calculated.

2.5. Model evaluation

In this study, 10-fold cross validation (CV) and leave-one-out cross validation (LOO-CV) methods were employed to evaluate the model performance as these method has the ability to examine the model's predictive ability (Beckerman et al., 2013).

The 10-fold cross validation was accomplished by splitting all data into 10 equal-sized folds. Subsequently, one of the folds was used to test the model, and the remaining 9 folds were used to train the model (Kim, 2009; Refaeilzadeh et al., 2009). This process was repeated 10 times for each model while all folds were used as the test subset and the R^2 and RMSE obtained from all models were averaged to calculate the final statistics (Dirgawati et al., 2015; Refaeilzadeh et al., 2009).

With LOO-CV technique, one monitoring site was left out and the model was fitted using the training sets derived from other sites (Brauer et al., 2003; Hochadel et al., 2006). Then, the model was used to predict the concentrations at the left out site and calculate the R^2 and RMSE values. This procedure was replicated while all sites were used once as the left out sample. Finally, the results were averaged to calculate the overall R^2 and RMSE.

We used R v.3.2.3 (R Foundation for Statistical Computing, Vienna, Austria) and MATLAB R2014b (MathWorks Inc., Natick, USA) for all statistical and soft computing analyses and ArcGIS version 10.2 (ESRI Inc., Redlands, USA) for spatial data processing and map creation.

3. Results

3.1. Modeling results

In this study, a wide range of ground-based NO_2 measurements, land use, meteorological, and satellite data were employed to estimate NO_2 concentration using ANFIS, as described in subsection 2.4. The effect of satellite and traffic variables on NO_2 estimations were evaluated. For this purpose, four different combinations of the variables were created and used for modelling process. The first model (model A) consisted of the meteorological and land use (spatial) variables. Satellite-based variables (NDVI and OMI tropospheric NO_2 column density) were included in the previous variables to create model B. With model C; the traffic variables (TRFL and CONF; described in Section 2.2) were replaced with road density variables (the sum of minor and major roads' length) used in model B. Finally, all effective spatial and spatiotemporal variables were included in model D.

For all models, the most effective predictors were determined using input selection process described in subsection 2.3. The results of the variable selection process are provided in the supplement (Table S1). Then, ANFIS was used to estimate the NO_2 concentration, and 10-fold CV and LOO-CV methods were also employed for assessing the model's generalization. Table 2 summarizes the R^2 and RMSE values obtained from model fitting and cross validation.

Model A consisted of the land use (spatial) and meteorological variables, and was able to explain 70% of the NO_2 variations, but it has the highest RMSE among the other models (2.79 ppb). The satellite (spatiotemporal) variables included in model B increased the R^2 by 14%, and decreased the RMSE by 28% compared to model A.

Using traffic variables rather than the road density in model C, R^2 increased by 5% and RMSE decreased by 18% compared to model B. Moreover, cross validation analyses showed that traffic variables increased the model's generality, and model C is less over-fitted compared

to model B due to the small difference between R^2 and RMSE values obtained from model fitting and cross validation analyses. Finally, model D which included all spatial and spatiotemporal variables had the best performance across ANFIS runs with lowest RMSE and highest R^2. Cross validation results also indicated that the data set used in model D increased the spatial predictive ability and model's generality.

Table 2. R-squared and RMSE for model fittings vs. cross validation

	Variables	Model		10-fold CV		LOO-CV	
		R^2	RMSE (ppb)	R^2	RMSE (ppb)	R^2	RMSE (ppb)
Model A	WS[a], LU[b],	0.70	2.79	0.66	2.91	0.58	4.28
Model B	WS, LU, satellite[c]	0.84	2.01	0.76	2.43	0.72	2.98
Model C	WS, satellite, IND[d], traffic[e]	0.89	1.64	0.87	1.70	0.81	2.21
Model D	WS, satellite, IND, traffic, minor road[f]	0.91	1.49	0.88	1.69	0.86	2.20

[a] Wind speed
[b] LU means the land use variables including the sum of industrial land use area within a 400m buffer, and the sum of minor and major roads' length within 800m, and 500m buffers respectively.
[c] The satellite variables include NDVI, and OMI tropospheric NO_2 column density.
[d] IND means the sum of industrial land use area within a 400m buffer.
[e] The traffic variables include the frequency of the congestion occurrence within a 1000m buffer and the sum of traffic-length interaction values within a 500m buffer.
[f] The minor road variable includes the sum of minor roads' length within a 800m buffer.

We compared the observed NO_2 concentrations to the predicted values of the model A, model B, model C, and model D (Figure 3). The predicted-observed plot of the model D indicates that the values are more equally scattered across the line of agreement at the low and high NO_2 concentrations compared to other models. In addition, the predicted-observed plot shows relatively weak correlation between predictions of the model A and actual observations.

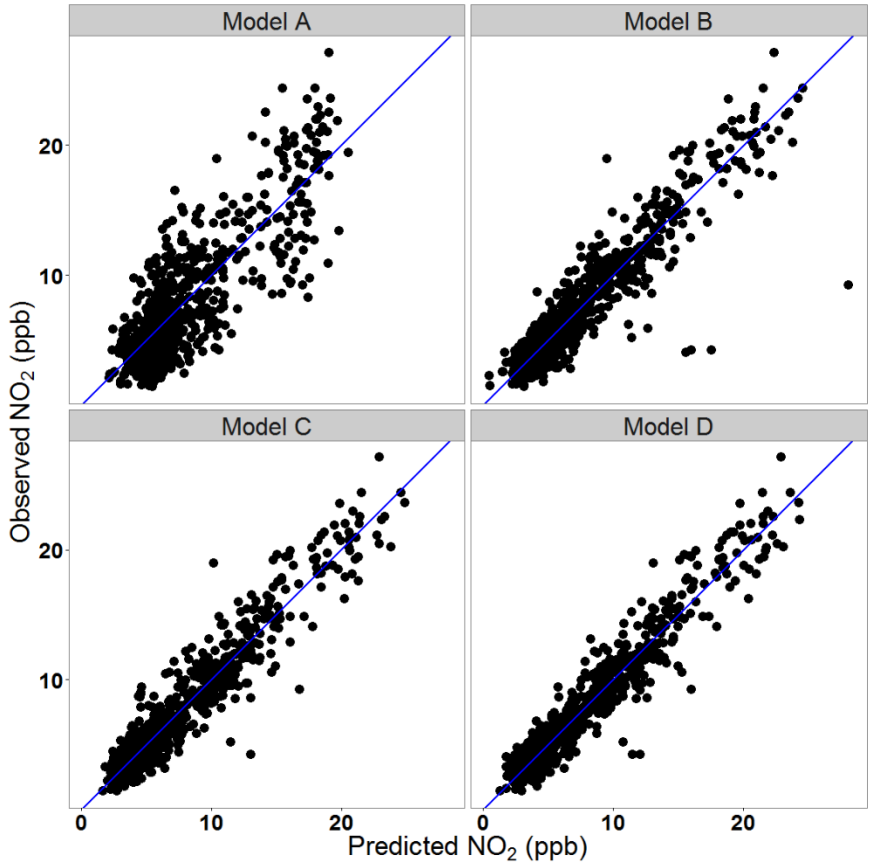

Figure 3. Scatter plots of predicted vs. observed NO_2 concentration for model A, B, C and D in SEQ. Blue line indicates the line of agreement (y=x).

Bland-Altman analysis was used to evaluate the agreement between the observation and predictions of model A, B, C, and D (Figure 4). The Bland-Altman plots demonstrated low bias in all models. However, model D predictions had the best agreement with the observations, and the fewest large residuals among other models.

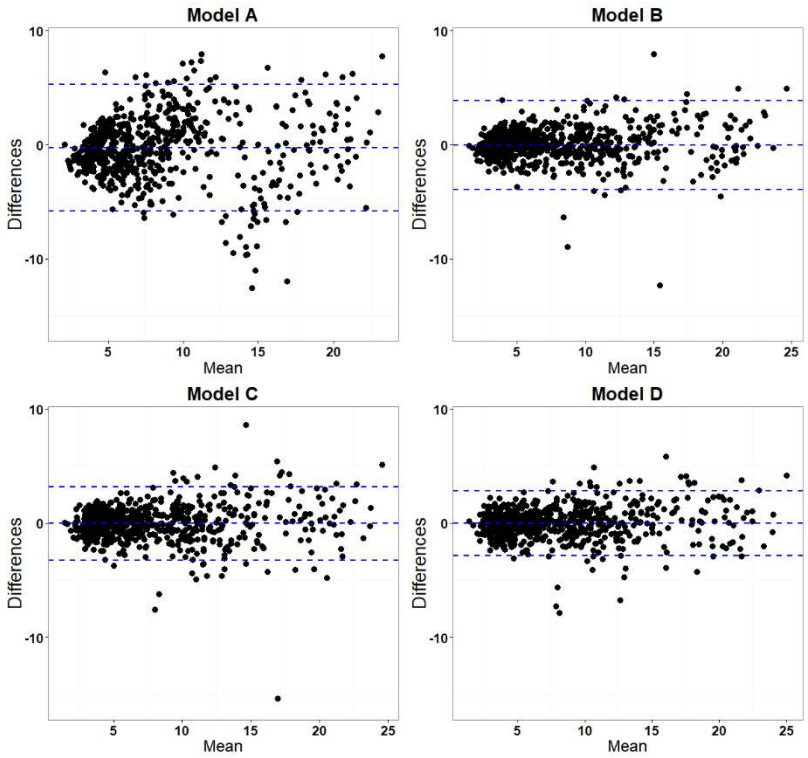

Figure 4. Bland-Altman plots of predicted and observed NO_2 concentrations (ppb).

In addition, a conventional land use regression (LUR) model has been used to predict the NO_2 concentration, and compare the prediction ability of the ANFIS and multiple regression, which is mostly used in conventional LUR models. Hence, the optimum dataset used in model D were utilized for training both models, and NO_2 concentrations were then predicted. A summary of the observed and predicted NO_2 concentrations is presented in Figure 5.

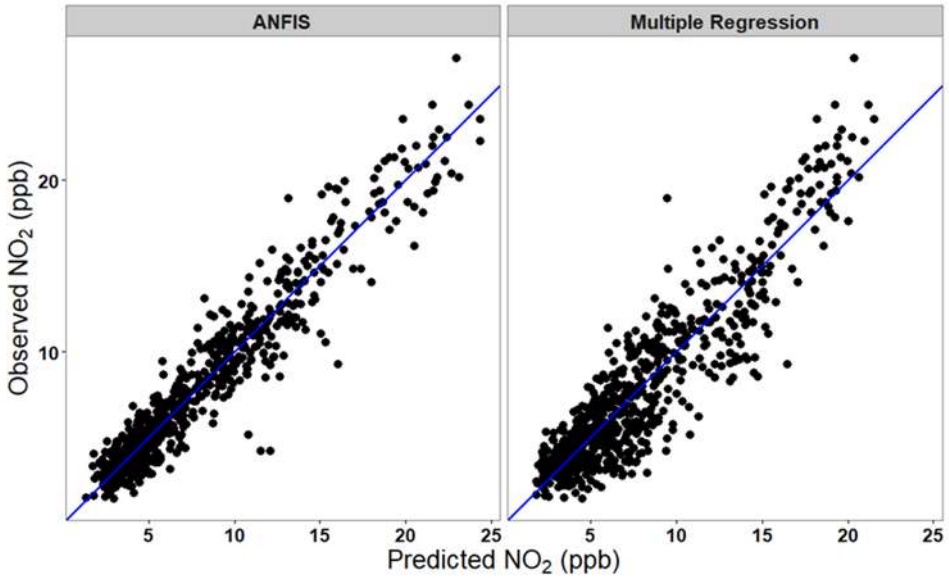

Figure 5. Scatter plots of predicted vs. observed NO_2 concentration for ANFIS and multiple regression in SEQ. Blue line indicates the line of agreement (y=x).

Table 3 compares the R^2 and RMSE for model fitting and cross validation results. For the model fit the R^2 values are 0.91 and 0.82 for the ANFIS and multiple regression models, respectively. The RMSE values are 1.49 ppb and 2.09 ppb for the ANFIS and multiple regression models, respectively. Compared with the multiple regression model, the ANFIS model could capture more variability (9%), while its RMSE decreased by 28%.

Comparing the difference between R^2 values derived from model fittings and cross validations results showed that the multiple regression model overfits more than ANFIS model. This also indicated that the ANFIS model had higher predictive ability and model's generality compared with the multiple regression model.

Table 3. R^2 and RMSE for model fittings vs. cross validation

	Model		10-fold CV		LOO-CV	
	R^2	RMSE (ppb)	R^2	RMSE (ppb)	R^2	RMSE (ppb)
ANFIS	0.91	1.49	0.88	1.69	0.86	2.20
Multiple Regression	0.82	2.09	0.79	2.17	0.66	3.88

3.2. Application of the model

To provide spatial estimates of NO_2 concentration, ANFIS model was applied to the centroid locations of the population grid in SEQ using the optimal subset of the predictors used in model D (best performance model).

Figure 6a illustrates the land use map of SEQ, and Figure 6b and 6c present the spatial distribution of annual average NO_2 concentration across SEQ in 2006 and 2011 respectively.

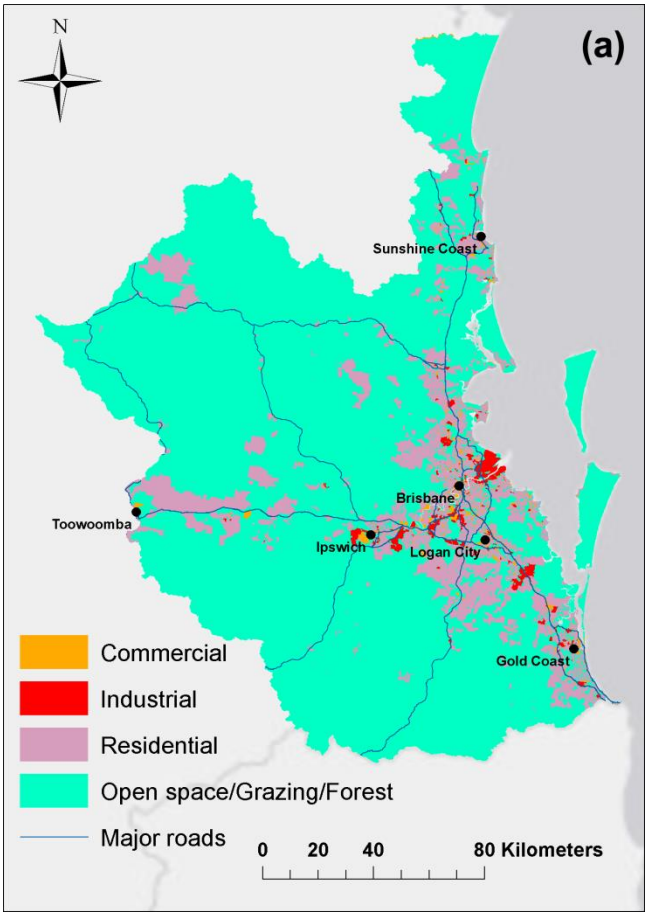
N
(a)
Sunshine Coast
Brisbane
Toowoomba
Ipswich
Logan City
Gold Coast
Commercial
Industrial
Residential
Open space/Grazing/Forest
Major roads
0 20 40 80 Kilometers

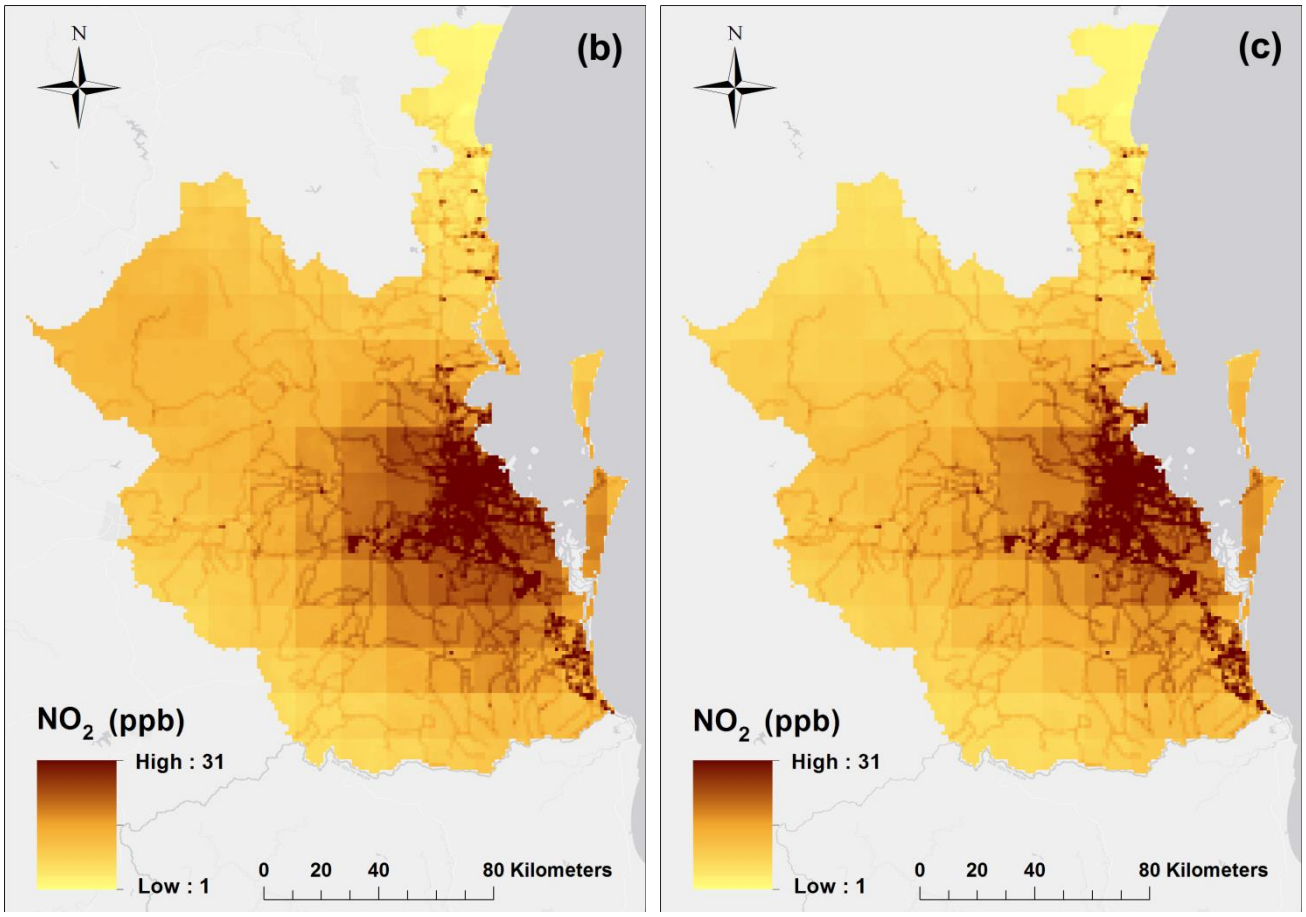

Figure 6. (a) Land use map of SEQ (b) Annual average NO_2 concentration in 2006 (c) Annual average NO_2 concentration in 2011.

In both years, concentration level ranged from 1 to 31 ppb. Areas with higher concentrations (20 to 31 ppb) corresponded to cities and major towns. Higher concentrations were predicted in locations with extensive adjacent industrial areas and major roads. This pattern was observed in all 6 cities of the study area. The highest levels were predicted for the three largest cities: Brisbane, Logan, and Ipswich. The annual average NO_2 concentration in 2006 and 2011 were calculated to compare the concentration levels in 5 local urban centres located in the study area.

Figure 7 shows the annual average NO_2 concentration levels in 5 local urban centres in 2006 and 2011. In general, the annual average concentration dropped from 7.5 ppb in 2006 to 6.4 ppb in 2011. The most significant reduction of NO_2 concentration was observed in Ipswich by 18.3%, and the least significant, at the Sunshine Coast by 6.6%. Also, the highest and the lowest average NO_2 concentrations were predicted in Brisbane and the Sunshine Coast respectively.

Figure 7. Summary of the predicted NO_2 concentration in 5 major cities in 2006 and 2011.

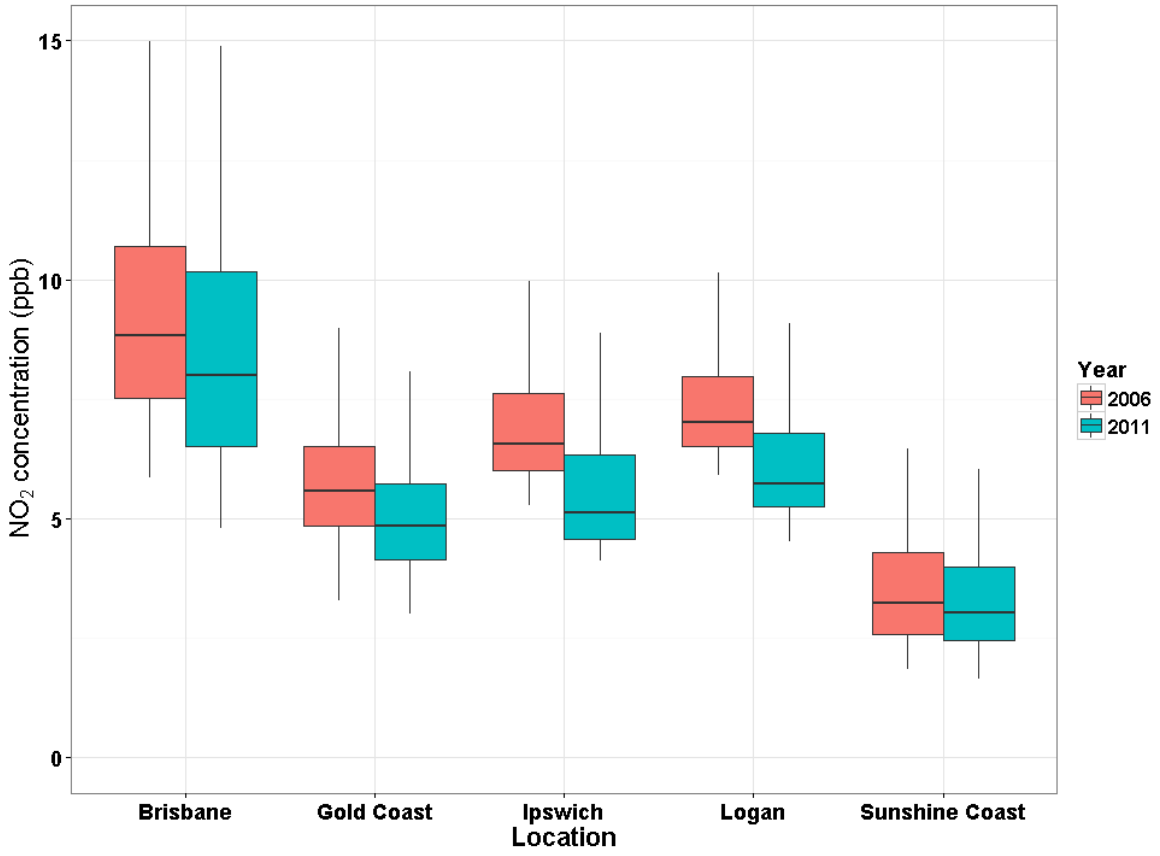

Population-weighted NO_2 concentrations were also calculated in local urban centres across SEQ. Using ANFIS model, the annual NO_2 concentrations were predicted at the centroids of the Australian population grid (1 km × 1 km grid) provided by Australian Bureau of Statistics (2011). The population density of each grid was multiplied by the predicted NO_2 concentration for each grid and the sum of this value for all grids was calculated and divided by the total population to calculate the population-weighted concentration. Table 4 summarized the population-weighted annual average NO_2 concentration in urban areas of SEQ in 2011.

Maximum and minimum average exposure to NO_2 was observed in Brisbane (9.65 ppb/km^2) and Sunshine Coast (3.83 ppb/km^2) respectively.

Table 4. Mean and population-weighted mean NO_2 concentration in urban areas of SEQ cities in 2011.

Location	Mean concentration (ppb)	Population-weighted mean concentration (ppb/km^2)
Brisbane	8.91	9.65
Gold Coast	5.2	5.82
Ipswich	6.06	6.51
Logan	6.37	7.45
Sunshine Coast	3.36	3.83

Figure 8 illustrates the seasonal predictions of NO_2 concentration in 2006. Mean predicted concentrations (ppb) were higher in Winter (6.56 ppb) and Autumn (4.35 ppb) than for Spring (4.24 ppb) and Summer (2.98 ppb). Maximum and minimum monthly average NO_2 concentrations were predicted in July (6.89 ppb), and February (2.58 ppb) respectively. Monthly prediction maps for 2006 and 2011 are given in the supplement (Figures S2 and S3).

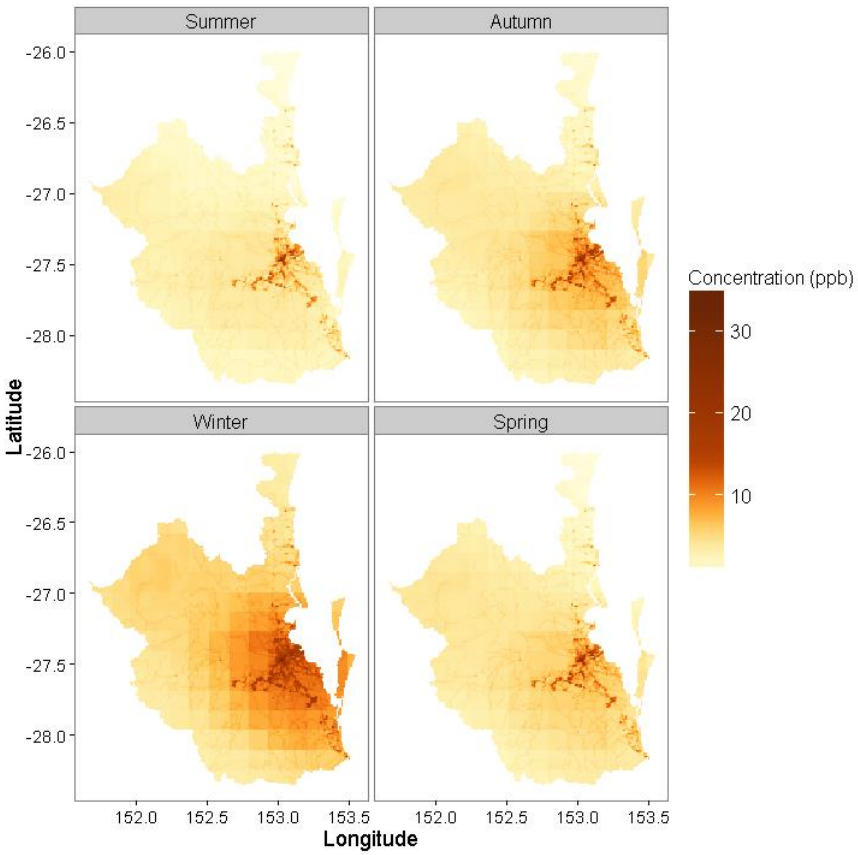

Figure 8. Seasonal average NO_2 concentrations in 2006.

4. Discussion

We employed ANFIS to improve the spatiotemporal modelling of NO_2 concentration using satellite, meteorological, land use, and traffic variables in South-east Queensland, Australia. To our knowledge this study used the ANFIS model to estimate NO_2 concentration for the first time. Using a cross validation technique, the ANFIS results were found to have good agreement with the NO_2 measurements. The results provide estimates of monthly and annually NO_2 concentrations for SEQ from 2006 to 2011. 10-fold CV and LOO-CV methods were employed to evaluate the predictive ability of the different combination of the predictors. Both CV methods used similar types of predictors for each model (model A, B, C, and D). Unlike LOO-CV, the 10-fold CV used some training sets derived from the left-out site to make its

predictions, hence higher R^2 and lower RMSE were obtained from 10-fold CV compared to LOO-CV results.

In this research, SEQSTM was used to calculate TRFL, and CONF. Both parameters were highly associated with NO_2 concentration across ANFIS runs. The WRF model was also employed to calculate PBLH, and WS. Based on the input selection results, WS was among the important predictors for estimating NO_2 concentration.

Prior studies mostly considered spatial predictors focused on road density and population-related data. Recent studies demonstrated that meteorological parameters could considerably affect the NO_2 concentrations (Elminir, 2005; Kim and Guldmann, 2011, 2015), hence we evaluated spatiotemporal predictors including satellite, meteorological, and traffic data in order to improve the temporal resolution of NO_2 estimates. Based on results summarized in Table 2, a comparison of the model mainly fed with spatial data (model A) and a model which used a combination of spatial and spatiotemporal data (model D) reveals an interesting finding. Adding the spatiotemporal data components to spatial data substantially improved the modelling accuracy and performance as RMSE decreased by 47% and R^2 increased by 21% (Figure 3). In addition, cross validation results showed model D was less overfit than model A, which means model A is not as general as model D.

The ANFIS model was found to have better performance and higher accuracy compared with multiple regression model, and better agreement with the observed data. Our results also corroborated with Sorek-Hamer et al. (2013) who showed that non-linear models like ANFIS have higher predictive ability compared with multiple regression model used in conventional LUR.

The results obtained from model A and model B show that including satellite-based variables increased the R^2 by 14%, and decreased the RMSE by 28%, which indicates the key role of satellite-based data in model's performance. In addition, Table 2 shows that the use of traffic

data (model C) rather than road density data (model B) decreased RMSE by 18% and increased R^2 by 5%. These results support the concept that traffic data derived from transport models provide more reliable information about traffic dynamics compared to traditional measures of traffic such as road density. In general, our results corroborate previous research recommending the use of spatiotemporal variables for NO_2 prediction (Bechle et al., 2015; Dirgawati et al., 2015; Gulliver et al., 2013; Vienneau et al., 2013), but also demonstrate an improved performance when spatiotemporal data is used to estimate the NO_2 concentration including satellite and traffic data.

Data sets with different spatial resolutions have been used in our study. The resolution of NDVI and WRF outputs, for example, is finer than the OMI satellite data. Individually, OMI tropospheric NO_2 column density data is provided at a coarse spatial resolution which is not accurate enough for assessing the exposure to NO_2 in epidemiological studies. However, method of combining different buffer sizes of land use parameters with meteorological, traffic and satellite-based data enabled the model to combine fine and more spatially coarse data sets to estimate NO_2 concentration and provide more informative results for epidemiological studies. These findings corroborate the result of other studies showing the advantages of combining several data with different spatiotemporal resolutions (Reid et al., 2015; Reis et al., 2015).

Another important finding was that the average NO_2 concentration levels were higher in 2006 compared to 2011 which could be due to the difference in vehicle emission standards in Australia. Prior to 2006, Euro 3 standard was applied to passenger vehicles and trucks in SEQ, while then any new vehicle manufactured after 2006 complied with Euro 4 standard in which lower level of NO_2 emission is permitted.

Different methodologies make it difficult to compare our results to other studies, however we have attempted to compare our results with other studies which have demonstrated the ability of statistical models for predicting NO_2 concentration (Dirgawati et al., 2015; Lee et al., 2014; Rahman et al., 2017). These studies developed LUR models to estimate the variation of NO_2, and reported R^2 lower than 0.75. Our model performed better than these models, which can be due to either: (1) the comprehensive input variables used or (2) spatiotemporal modelling approach or (3) the more robust modeling algorithm used.

There are some limitations attributed to the data availability in this study, consequently 9% of the NO_2 variations were unexplained by the ANFIS model. The number of observations plays a key role in statistical models (Basagaña et al., 2012). Therefore special attention has been paid to the number of observations. The use of the temporal data provided further variability for air quality measurements in this study. The number of observations used in this study was enough to meet the minimum requirements suggested by Basagaña et al. (2012), but sparse spatial distribution of the monitoring sites in the study area remain as a limitation of this study.

Although the traffic congestion found to be a better metrics for the traffic data compared with the road density, the use of SEQSTM limited our model, as SEQSTM provided only the annual average congestion, which smoothed out the monthly variation of the congestion data. Another issue was that the concentrations were measured from 2006 to 2011, while the land use parameters were only available for 2011.

Moreover, the type of the air quality monitoring stations was not included as a potential predictor. Levy et al. (2015) suggested that including this predictor could improve the performance of LUR model. Aura passes over SEQ at 14 pm, hence the OMI tropospheric NO_2 column density might underestimate the actual NO_2 concentration due to the high rate of the photochemical reactions in the atmosphere at this hour of the day. The cloud cover during a proportion of the Austral summer

resulted in missing satellite data, hence the modelling outputs may be affected by the loss of the satellite data during the Austral summer.

5. Conclusions

In this study, a satellite-based model was developed for estimating the spatiotemporal variation of NO_2 concentration on a monthly base. An ANFIS model used for predicting NO_2 concentration performed very well and exhibited satisfactory performance with R^2, and RMSE equal to 0.91, and 1.49 ppb, respectively. It provided estimates of monthly and annually NO_2 concentrations during 2006-2011. The traffic and satellite data used in this study was found to enhance the estimation of NO_2 concentrations. The method of combining spatiotemporal data with different resolution, such as that from satellite, traffic, and meteorological data with local land use parameters significantly improved the model's performance, and provided more informative results. This novel approach can be applied to precisely estimate the NO_2 concentration in different environments. The model is particularly useful for epidemiological studies and other researches looking for accurate estimates of NO_2 concentration at different times. Finally, our study demonstrates the great potential of the ANFIS model trained by traffic data incorporated with satellite, meteorological, and land use data to improve the accuracy of spatiotemporal NO_2 estimations. Further analysis such as sensitivity and uncertainty analyses can also be done to assess the importance of input parameters and uncertainty in the modelling results.

Acknowledgment

A PhD scholarship to Bijan Yeganeh has been provided by the Centre for Air Quality & Health Research and Evaluation (National Health and Medical Research Council Centre of Research Excellence). We thank the scientists and staff of NASA for the Aura mission as well

as the Finnish Meteorological Institute and the Netherlands Agency for Aerospace Programs for the OMI sensor. We also thank the Australian Government, Bureau of Meteorology, NASA/NOAA, Australian National Pollutant Inventory, Australian Bureau of Statistics, CSIRO and the Terrestrial Ecosystem Research Network for Auscover land use, NDVI and related data sets. We thank the Queensland Government for NO_2 data, and Department of Transport and Main Roads for providing the SEQSTM's result. WRF was processed on the National Computational Infrastructure (NCI) facility in Canberra, Australia, which is supported by the Australian Government.

References

Agirre-Basurko, E., Ibarra-Berastegi, G., Madariaga, I., 2006. Regression and multilayer perceptron-based models to forecast hourly O_3 and NO_2 levels in the Bilbao area. Environmental Modelling & Software 21(4) 430-446.

Al-Alawi, S.M., Abdul-Wahab, S.A., Bakheit, C.S., 2008. Combining principal component regression and artificial neural networks for more accurate predictions of ground-level ozone. Environmental Modelling & Software 23(4) 396-403.

Amini, M., Abbaspour, K.C., Berg, M., Winkel, L., Hug, S.J., Hoehn, E., Yang, H., Johnson, C.A., 2008. Statistical modeling of global geogenic arsenic contamination in groundwater. Environmental Science & Technology 42(10) 3669-3675.

Australian Bureau of Statistics, 2011. Australian Statistical Geography Standard, Volume 1. , Main Structure and Greater Capital City Statistical Areas: Canbrra, Australia, p. 15.

Australian Bureau of Statistics., 2011. Australian Population Grid, 1 ed. Australian Government: Australia.

Australian Bureau of Statistics., 2012. Population Change in South-East Queensland: Australia.

Australian Government, 2010. Air quality fact sheet, Nitrogen dioxide (NO_2). Department of the Environment and Heritage: Australia.

Basagaña, X., Rivera, M., Aguilera, I., Agis, D., Bouso, L., Elosua, R., Foraster, M., de Nazelle, A., Nieuwenhuijsen, M., Vila, J., 2012. Effect of the number of measurement sites on land use regression models in estimating local air pollution. Atmospheric Environment 54 634-642.

Bechle, M.J., Millet, D.B., Marshall, J.D., 2015. National Spatiotemporal Exposure Surface for NO_2: Monthly Scaling of a Satellite-Derived Land-Use Regression, 2000–2010. Environmental Science & Technology 49(20) 12297-12305.

Beckerman, B.S., Jerrett, M., Martin, R.V., van Donkelaar, A., Ross, Z., Burnett, R.T., 2013. Application of the deletion/substitution/addition algorithm to selecting land use regression models for interpolating air pollution measurements in California. Atmospheric Environment 77 172-177.

Brauer, M., Hoek, G., van Vliet, P., Meliefste, K., Fischer, P., Gehring, U., Heinrich, J., Cyrys, J., Bellander, T., Lewne, M., 2003. Estimating long-term average particulate air pollution concentrations: application of traffic indicators and geographic information systems. Epidemiology 14(2) 228-239.

Briggs, D.J., Collins, S., Elliott, P., Fischer, P., Kingham, S., Lebret, E., Pryl, K., van Reeuwijk, H., Smallbone, K., Van Der Veen, A., 1997. Mapping urban air pollution using GIS: a regression-based approach. International Journal of Geographical Information Science 11(7) 699-718.
Bureau of Meteorology, 2015. Normalised Difference Vegetation Index: Australia.
Bureau of Transport and Regional Economics., 2007. Estimating urban traffic and congestion cost trends for Australian cities. working paper 71, Canberra , Australia.
Carnevale, C., Finzi, G., Pederzoli, A., Turrini, E., Volta, M., 2016. Lazy Learning based surrogate models for air quality planning. Environmental Modelling & Software 83 47-57.
Corani, G., Scanagatta, M., 2016. Air pollution prediction via multi-label classification. Environmental Modelling & Software 80 259-264.
Costabile, F., Allegrini, I., 2008. A new approach to link transport emissions and air quality: An intelligent transport system based on the control of traffic air pollution. Environmental Modelling & Software 23(3) 258-267.
Crouse, D.L., Goldberg, M.S., Ross, N.A., Chen, H., Labrèche, F., 2010. Postmenopausal breast cancer is associated with exposure to traffic-related air pollution in Montreal, Canada: a case-control study. Environmental health perspectives 118(11) 1578.
Crouse, D.L., Peters, P.A., Villeneuve, P.J., Proux, M.-O., Shin, H.H., Goldberg, M.S., Johnson, M., Wheeler, A.J., Allen, R.W., Atari, D.O., 2015. Within-and between-city contrasts in nitrogen dioxide and mortality in 10 Canadian cities; a subset of the Canadian Census Health and Environment Cohort (CanCHEC). Journal of Exposure Science and Environmental Epidemiology 25(5) 482-489.
Davis, P., Peckham, M., 2007. The Analysis of Gasolline Transient Emissions ehaviour Using East: Response Gas Anallyseirs. SAE Technical Papers 2007-2026-2015.
Derwent, R.G., Hertel, O., 1998. Transformation of air pollutants, Urban Air Pollution - European Aspects. Springer: UK, pp. 137-159.
Dirgawati, M., Barnes, R., Wheeler, A.J., Arnold, A.-L., McCaul, K.A., Stuart, A.L., Blake, D., Hinwood, A., Yeap, B.B., Heyworth, J.S., 2015. Development of Land Use Regression models for predicting exposure to NO_2 and NOx in Metropolitan Perth, Western Australia. Environmental Modelling & Software 74 258-267.
Ducret-Stich, R.E., Tsai, M.-Y., Ragettli, M.S., Ineichen, A., Kuenzli, N., Phuleria, H.C., 2013. Role of highway traffic on spatial and temporal distributions of air pollutants in a Swiss Alpine valley. Science of the Total Environment 456 50-60.
Eeftens, M., Beelen, R., Fischer, P., Brunekreef, B., Meliefste, K., Hoek, G., 2011. Stability of measured and modelled spatial contrasts in NO_2 over time. Occupational and Environmental Medicine 68(10) 765-770.
Elminir, H.K., 2005. Dependence of urban air pollutants on meteorology. Science of the Total Environment 350(1) 225-237.
Evans, R.J., Burke, M.I., Dodson, J.R., 2007. Clothing the Emperor?: Transport modelling and decision-making in Australian cities, Proceedings of State of Australian Cities National Conference 2007.
Filleul, L., Rondeau, V., Vandentorren, S., Le Moual, N., Cantagrel, A., Annesi-Maesano, I., Charpin, D., Declercq, C., Neukirch, F., Paris, C., 2005. Twenty five year mortality and air pollution: results from the French PAARC survey. Occupational and Environmental Medicine 62(7) 453-460.
Forouzanfar, M.H., Alexander, L., Anderson, H.R., Bachman, V.F., Biryukov, S., Brauer, M., Burnett, R., Casey, D., Coates, M.M., Cohen, A., 2015. Global, regional, and national comparative risk assessment of 79 behavioural, environmental and occupational, and metabolic risks or clusters of risks in 188 countries, 1990–2013: a systematic analysis for the Global Burden of Disease Study 2013. The Lancet 386(10010) 2287-2323.

Giakoumis, E.G., Rakopoulos, C.D., Dimaratos, A.M., Rakopoulos, D.C., 2012. Exhaust emissions of diesel engines operating under transient conditions with biodiesel fuel blends. Progress in Energy and Combustion Science 38(5) 691-715.
Grundström, M., Hak, C., Chen, D., Hallquist, M., Pleijel, H., 2015. Variation and co-variation of PM_{10}, particle number concentration, NOx and NO_2 in the urban air–Relationships with wind speed, vertical temperature gradient and weather type. Atmospheric Environment 120 317-327.
Gulliver, J., De Hoogh, K., Hansell, A., Vienneau, D., 2013. Development and back-extrapolation of NO_2 land use regression models for historic exposure assessment in Great Britain. Environmental Science and Technology 47(14) 7804-7811.
Hagena, J.R., Filipi, Z.S., Assanis, D.N., 2006. Transient diesel emissions: Analysis of engine operation during a tip-in. SAE Technical Papers 2006-2001-1151.
Henderson, S.B., Beckerman, B., Jerrett, M., Brauer, M., 2007. Application of land use regression to estimate long-term concentrations of traffic-related nitrogen oxides and fine particulate matter. Environmental Science & Technology 41(7) 2422-2428.
Hochadel, M., Heinrich, J., Gehring, U., Morgenstern, V., Kuhlbusch, T., Link, E., Wichmann, H.-E., Krämer, U., 2006. Predicting long-term average concentrations of traffic-related air pollutants using GIS-based information. Atmospheric Environment 40(3) 542-553.
Hoek, G., Eeftens, M., Beelen, R., Fischer, P., Brunekreef, B., Boersma, K.F., Veefkind, P., 2015. Satellite NO_2 data improve national land use regression models for ambient NO_2 in a small densely populated country. Atmospheric Environment 105 173-180.
Hojati, A.T., Ferreira, L., Washington, S., Charles, P., Shobeirinejad, A., 2014. Modelling total duration of traffic incidents including incident detection and recovery time. Accident Analysis & Prevention 71 296-305.
Horsburgh, J.S., Aufdenkampe, A.K., Mayorga, E., Lehnert, K.A., Hsu, L., Song, L., Jones, A.S., Damiano, S.G., Tarboton, D.G., Valentine, D., 2016. Observations Data Model 2: A community information model for spatially discrete Earth observations. Environmental Modelling & Software 79 55-74.
Hystad, P., Setton, E., Cervantes, A., Poplawski, K., Deschenes, S., Brauer, M., van Donkelaar, A., Lamsal, L., Martin, R., Jerrett, M., Demers, P., 2011. Creating National Air Pollution Models for Population Exposure Assessment in Canada. Environmental health perspectives 119(8) 1123-1129.
Jang, J.-S.R., 1991. Fuzzy Modeling Using Generalized Neural Networks and Kalman Filter Algorithm, AAAI, pp. 762-767.
Jang, J.-S.R., 1993. ANFIS: adaptive-network-based fuzzy inference system. Systems, Man and Cybernetics, IEEE Transactions on 23(3) 665-685.
Jang, J.-S.R., Gulley, N., 1995. The fuzzy logic toolbox for use with MATLAB. The Mathworks Inc.
Jones, D.A., Wang, W., Fawcett, R., 2009. High-quality spatial climate data-sets for Australia. Australian Meteorological and Oceanographic Journal 58(4) 233.
Keuken, M., Jonkers, S., Wilmink, I., Wesseling, J., 2010. Reduced NOx and PM_{10} emissions on urban motorways in The Netherlands by 80km/h speed management. Science of the Total Environment 408(12) 2517-2526.
Kim, J.-H., 2009. Estimating classification error rate: Repeated cross-validation, repeated hold-out and bootstrap. Computational Statistics & Data Analysis 53(11) 3735-3745.
Kim, Y., Guldmann, J.-M., 2011. Impact of traffic flows and wind directions on air pollution concentrations in Seoul, Korea. Atmospheric Environment 45(16) 2803-2810.
Kim, Y., Guldmann, J.-M., 2015. Land-use regression panel models of NO_2 concentrations in Seoul, Korea. Atmospheric Environment 107 364-373.

Kloog, I., Chudnovsky, A.A., Just, A.C., Nordio, F., Koutrakis, P., Coull, B.A., Lyapustin, A., Wang, Y., Schwartz, J., 2014. A new hybrid spatio-temporal model for estimating daily multi-year $PM_{2.5}$ concentrations across northeastern USA using high resolution aerosol optical depth data. Atmospheric Environment 95 581-590.
Klop, J., Guderian, E., 2008. Linking of Mobility Performance Measures to Resource Allocation: Survey of State DOTS and MPOS. Colorado Department of Transportation, DTD Applied Research and Innovation Branch: USA.
Knibbs, L.D., Hewson, M.G., Bechle, M.J., Marshall, J.D., Barnett, A.G., 2014. A national satellite-based land-use regression model for air pollution exposure assessment in Australia. Environmental research 135 204-211.
Kruse, R., Pasi, G., Alonso, J.M., 2013. Introduction to the Soft Computing and Intelligent Data Analysis Minitrack, 46th Hawaii International Conference on System Sciences, p. 1384.
Lee, J.-H., Wu, C.-F., Hoek, G., de Hoogh, K., Beelen, R., Brunekreef, B., Chan, C.-C., 2014. Land use regression models for estimating individual NO x and NO 2 exposures in a metropolis with a high density of traffic roads and population. Science of the Total Environment 472 1163-1171.
Levelt, P.F., Van den Oord, G.H., Dobber, M.R., Malkki, A., Visser, H., De Vries, J., Stammes, P., Lundell, J.O., Saari, H., 2006. The ozone monitoring instrument. IEEE Transactions on geoscience and remote sensing 44(5) 1093-1101.
Levy, I., Levin, N., Schwartz, J.D., Kark, J.D., 2015. Back-extrapolating a land use regression model for estimating past exposures to traffic-related air pollution. Environmental Science & Technology 49(6) 3603-3610.
Lin, C.-T., Lee, C.S.G., 1991. Neural-network-based fuzzy logic control and decision system. IEEE Transactions on computers 40(12) 1320-1336.
Lomax, T.J., 1997. Quantifying congestion (No. 398). Transportation Research Board, Washington D.C. , USA.
Luk, J., Kazantzidis, G., Han, C., 2009. Estimating road network congestion and associated costs, In: Austroads (Ed.). Austroads publication: Sydney, Australia.
Martin, R.V., 2008. Satellite remote sensing of surface air quality. Atmospheric Environment 42(34) 7823-7843.
Mathur, N., Glesk, I., Buis, A., 2016. Comparison of adaptive neuro-fuzzy inference system (ANFIS) and Gaussian processes for machine learning (GPML) algorithms for the prediction of skin temperature in lower limb prostheses. Medical Engineering & Physics.
McBride, S.J., Williams, R.W., Creason, J., 2007. Bayesian hierarchical modeling of personal exposure to particulate matter. Atmospheric Environment 41(29) 6143-6155.
Moazami, S., Noori, R., Amiri, B.J., Yeganeh, B., Partani, S., Safavi, S., 2016. Reliable prediction of carbon monoxide using developed support vector machine. Atmospheric Pollution Research 7(3) 412-418.
Mölter, A., Agius, R., de Vocht, F., Lindley, S., Gerrard, W., Custovic, A., Simpson, A., 2014. Effects of long-term exposure to PM_{10} and NO_2 on asthma and wheeze in a prospective birth cohort. J Epidemiol Community Health 68(1) 21-28.
Mölter, A., Lindley, S., de Vocht, F., Simpson, A., Agius, R., 2010. Modelling air pollution for epidemiologic research - Part II: Predicting temporal variation through land use regression. Science of the Total Environment 409(1) 211-217.
Naji, S., Shamshirband, S., Basser, H., Alengaram, U.J., Jumaat, M.Z., Amirmojahedi, M., 2016. Soft computing methodologies for estimation of energy consumption in buildings with different envelope parameters. Energy Efficiency 9(2) 435-453.
NASA, 2007. Ozone Monitoring Instrument, Spacecraft and Instruments. NASA: USA.

Novotny, E.V., Bechle, M.J., Millet, D.B., Marshall, J.D., 2011. National satellite-based land-use regression: NO_2 in the United States. Environmental Science & Technology 45(10) 4407-4414.
Ordieres, J., Vergara, E., Capuz, R., Salazar, R., 2005. Neural network prediction model for fine particulate matter ($PM_{2.5}$) on the US–Mexico border in El Paso (Texas) and Ciudad Juárez (Chihuahua). Environmental Modelling & Software 20(5) 547-559.
Ovaska, S.J., 2004. Computationally Intelligent Hybrid Systems: The Fusion of Soft Computing and Hard Computing (IEEE Press Series on Computational Intelligence). Wiley-IEEE Press.
Parent, M.-É., Goldberg, M.S., Crouse, D.L., Ross, N.A., Chen, H., Valois, M.-F., Liautaud, A., 2013. Traffic-related air pollution and prostate cancer risk: a case–control study in Montreal, Canada. Occupational and Environmental Medicine 70(7) 511-518.
Perez, L., Lurmann, F., Wilson, J., Pastor, M., Brandt, S.J., Künzli, N., McConnell, R., 2012. Near-roadway pollution and childhood asthma: implications for developing'win-win'compact urban development and clean vehicle strategies. Environmental health perspectives: journal of the National Institute of Environmental Health Sciences 120 1619-1626.
Powers, G., Huang, X.-y., Klemp, B., Skamarock, C., Dudhia, J., Gill, O., Duda, G., Barker, D., Wang, W., 2008. A description of the Advanced Research WRF version 3.
Rahman, M.M., Yeganeh, B., Clifford, S., Knibbs, L.D., Morawska, L., 2017. Development of a land use regression model for daily NO_2 and NOx concentrations in the Brisbane metropolitan area, Australia. Environmental Modelling & Software 95 168-179.
Rakopoulos, C.D., Giakoumis, E.G., 2009. Diesel engine transient operation: principles of operation and simulation analysis. Springer Science & Business Media.
Refaeilzadeh, P., Tang, L., Liu, H., 2009. Cross-validation, Encyclopedia of database systems. Springer, pp. 532-538.
Reggente, M., Peters, J., Theunis, J., Van Poppel, M., Rademaker, M., Kumar, P., De Baets, B., 2014. Prediction of ultrafine particle number concentrations in urban environments by means of Gaussian process regression based on measurements of oxides of nitrogen. Environmental Modelling & Software 61 135-150.
Reid, C.E., Jerrett, M., Petersen, M.L., Pfister, G.G., Morefield, P.E., Tager, I.B., Raffuse, S.M., Balmes, J.R., 2015. Spatiotemporal Prediction of Fine Particulate Matter During the 2008 Northern California Wildfires Using Machine Learning. Environmental Science & Technology 49(6) 3887-3896.
Reis, S., Seto, E., Northcross, A., Quinn, N.W., Convertino, M., Jones, R.L., Maier, H.R., Schlink, U., Steinle, S., Vieno, M., 2015. Integrating modelling and smart sensors for environmental and human health. Environmental Modelling & Software 74 238-246.
Richter, A., Burrows, J.P., Nüß, H., Granier, C., Niemeier, U., 2005. Increase in tropospheric nitrogen dioxide over China observed from space. Nature 437(7055) 129-132.
Rose, N., Cowie, C., Gillett, R., Marks, G.B., 2010. Validation of a spatiotemporal land use regression model incorporating fixed site monitors. Environmental Science & Technology 45(1) 294-299.
Rose, N., Cowie, C., Gillett, R., Marks, G.B., 2011. Validation of a spatiotemporal land use regression model incorporating fixed site monitors. Environmental Science and Technology 45(1) 294-299.
Ryan, M., Cormack, S., Copland, A., 2008. BSTM Multi-Modal Model Development, Network and Zoning. Queensland government, Queensland transport main roads Working Paper 1, Queensland, Australia.
Sahsuvaroglu, T., Arain, A., Kanaroglou, P., Finkelstein, N., Newbold, B., Jerrett, M., Beckerman, B., Brook, J., Finkelstein, M., Gilbert, N.L., 2006. A land use regression model

for predicting ambient concentrations of nitrogen dioxide in Hamilton, Ontario, Canada. Journal of the Air & Waste Management Association 56(8) 1059-1069.
Sampson, P.D., Szpiro, A.A., Sheppard, L., Lindström, J., Kaufman, J.D., 2011. Pragmatic estimation of a spatio-temporal air quality model with irregular monitoring data. Atmospheric Environment 45(36) 6593-6606.
Shekarrizfard, M., Valois, M.-F., Goldberg, M.S., Crouse, D., Ross, N., Parent, M.-E., Yasmin, S., Hatzopoulou, M., 2015. Investigating the role of transportation models in epidemiologic studies of traffic related air pollution and health effects. Environmental research 140 282-291.
Sorek-Hamer, M., Strawa, A., Chatfield, R., Esswein, R., Cohen, A., Broday, D., 2013. Improved retrieval of $PM_{2.5}$ from satellite data products using non-linear methods. Environmental pollution 182 417-423.
Su, J., Jerrett, M., Beckerman, B., 2009. A distance-decay variable selection strategy for land use regression modeling of ambient air pollution exposures. Science of the Total Environment 407(12) 3890-3898.
The Mathworks Inc., 2005. Training routine for Sugeno-type fuzzy inference system: USA.
Torres, O., Tanskanen, A., Veihelmann, B., Ahn, C., Braak, R., Bhartia, P.K., Veefkind, P., Levelt, P., 2007. Aerosols and surface UV products from Ozone Monitoring Instrument observations: An overview. Journal of Geophysical Research-Atmospheres 112(D24).
Vienneau, D., de Hoogh, K., Bechle, M.J., Beelen, R., van Donkelaar, A., Martin, R.V., Millet, D.B., Hoek, G., Marshall, J.D., 2013. Western European land use regression incorporating satellite-and ground-based measurements of NO_2 and PM_{10}. Environmental Science & Technology 47(23) 13555-13564.
Weymouth, G., Le Marshall, J., 2001. Estimation of daily surface solar exposure using GMS-5 stretched-VISSR observations: the system and basic results. Australian Meteorological Magazine 50(4) 263.
Wu, Y., Guo, J., Zhang, X., Tian, X., Zhang, J., Wang, Y., Duan, J., Li, X., 2012. Synergy of satellite and ground based observations in estimation of particulate matter in eastern China. Science of the Total Environment 433 20-30.
Yeganeh, B., Hewson, M.G., Clifford, S., Knibbs, L.D., Morawska, L., 2017. A satellite-based model for estimating $PM_{2.5}$ concentration in a sparsely populated environment using soft computing techniques. Environmental Modelling & Software 88 84-92.
Yeganeh, B., Motlagh, M.S.P., Rashidi, Y., Kamalan, H., 2012. Prediction of CO concentrations based on a hybrid partial least square and support vector machine model. Atmospheric Environment 55 357-365.

Supplementary Material

Development of a Satellite-based Model for Estimating the Long-term Spatiotemporal Exposure to NO_2

Bijan Yeganeh[1, 2], Michael G. Hewson[3], Samuel Clifford[2, 4], Ahmad Tavassoli[5], Luke D. Knibbs[6], and Lidia Morawska[1]

[1] International Laboratory for Air Quality and Health, Queensland University of Technology, Brisbane, Queensland 4001, Australia

[2] Centre for Air quality and health Research and evaluation, Glebe, New South Wales 2037, Australia

[3] School of Education and the Arts, Central Queensland University, North Rockhampton, Queensland 4702, Australia

[4] ARC Centre of Excellence for Mathematical and Statistical Frontiers, Queensland University of Technology, Brisbane, Queensland 4001, Australia

[5] School of Civil Engineering, The University of Queensland, St Lucia, Queensland 4072, Australia

[6] School of Public Health, The University of Queensland, Herston, Queensland 4006, Australia

1. Modelled Planetary Boundary Layer Height and Wind Vectors

The Climate Research Group (CRG) of The University of Queensland (UQ) School of Geography, Planning and Environment Management provided the planetary boundary layer (PBL) height and wind vectors (U and V) for the spatial analysis of the project. The Weather Research and Forecasting model (WRF) was used to calculate daily at 2 pm Australian Eastern standard Time (AEST): (1) average PBL height in metres above ground level (AGL); and (2) 10 metre AGL wind vectors. These variables were averaged for each month for six years (2006 to 2011). The time of 14:00 AEST was chosen to coincide with the instrument ephemeris calculated Aura satellite overpass time for the study area.

1.1 Weather Model Configuration

WRF is a community "numerical weather prediction and atmospheric simulation system for both research and operational applications" (Skamarock et al., 2005) that has been evolving through predecessors for some twenty years. CRG used WRF version 3.5 for this work.

The WRF three dimensional, two domain configuration was designed considering model guiding documentation (Wang et al., 2012) and a project need to optimise model running time and still enable at least a moderate model output spatial resolution. The WRF nested domains were at a 5:1 (outer:inner) ratio as shown in Figure S1. The model domains were centred at latitude 27.5 degrees south and longitude 152 degrees east – just west of the project subject city of Brisbane. The outer domain had a spatial resolution of 15 km and the inner domain was therefore set at 3 km. The domain design, particularly the size of the outer domain, made optimal use of six-hourly Global Forecasting System (GFS) reanalysed meteorological data archive. The inner domain size of 3 km was chosen to resolve terrain features suitable to the GIS based multivariate analysis while not burdening the model run times unnecessarily. WRF earth surface database best spatial resolution is 30 arc-seconds so the inner domain spatial resolution matched the geographical initial condition data. While it has been shown that a WRF

1 km spatial resolution best accounts for topographic effects on wind flow (Horvath et al., 2012), the project selection of WRF wind vectors (U, V) at 10 metres above ground level combined with the 3 km spatial resoultion provided a suitable modelled wind surface to use in the GIS enabled multivariate spatial analsysis. The WRF inner domains was sized to 121 * 121 grid squares – greater than the minimum 100 * 100 grid square size recommended by WRF user guidance (Wang et al., 2012). The model tropospheric depth was divided into 30 sigma levels.

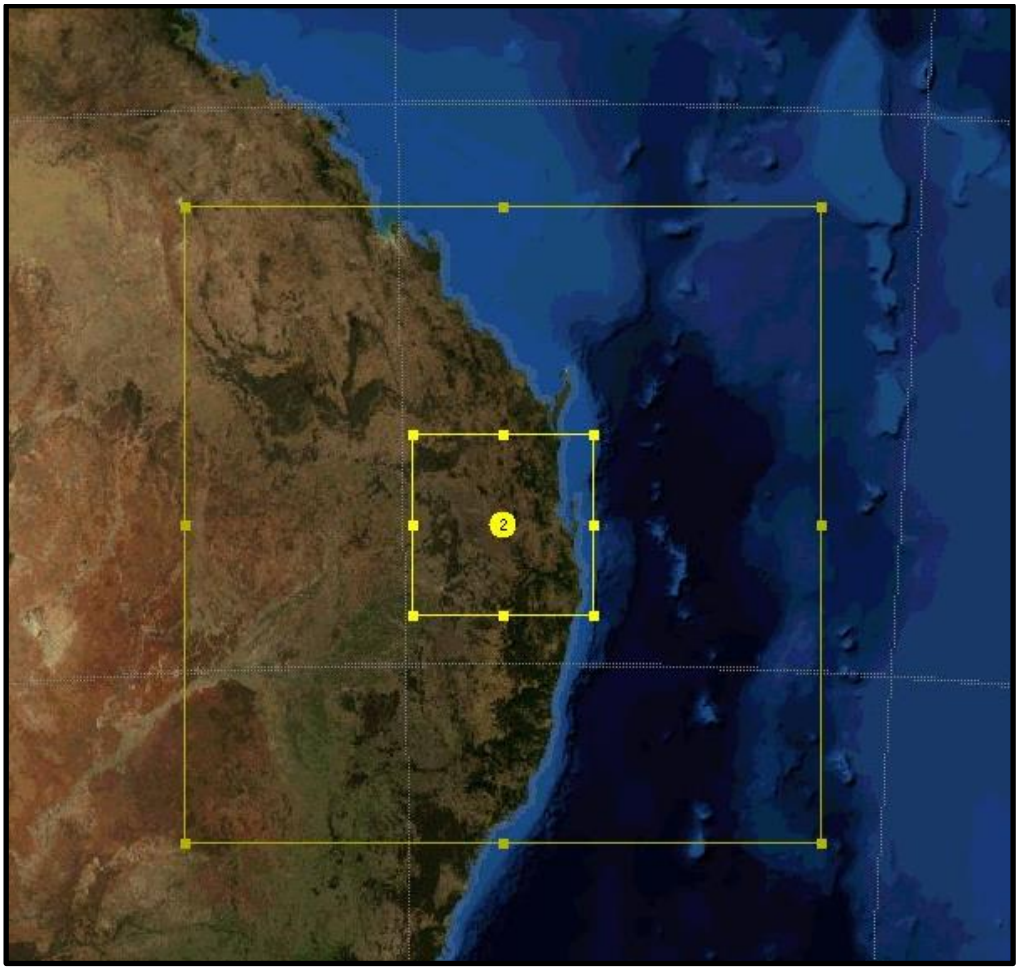

Figure S1: the WRF model two domain design centred on a location to the west of the Australian city of Brisbane at 27.5 south and 152 degrees east.

GFS 6 hourly, reanalysed meteorology data is provided by the US National Centre for Environmental Prediction (NCEP) as final operational global tropospheric analysis. Since this data incorporates weather observations at one degree latitude/longitude a large outer domain is needed so that sufficient meteorology is provided to the model boundary and initial conditions. WRF model geographical boundary and initial conditions created by the WRF Pre-processing System (WPS) were compiled from:

- United States Geological Survey (USGS) topography at 30 arc-seconds;
- USGS 24 land use categories;
- USGS 16 soil categories; and
- Standard WRF provided albedo, soil temperature, sea surface temperature and green fraction data sets.

WRF physics scheme configurations were chosen based on those found optimal for wind modelling (Deppe et al., 2013; Santos-Alamillos et al., 2013; Yang et al., 2013; Zhang et al., 2013) and suitable for Australian environmental conditions (Evans et al., 2012). The main physics scheme selections being:

- Microphysics – WSM (WRF single moment) 3-class;
- Longwave radiation – RRTM (Rapid Radiative Transfer Model) scheme;
- Shortwave scheme – Dudhia scheme;
- Surface layer option – Monin-Obukhov scheme;
- Land surface option – Unified Noah land-surface model;
- Boundary layer option – YSU (Yonsei University) scheme;
- Cumulus option (outer domain only) – Kain-Fritsch scheme; and
- Vertical velocity damping switched on.

1.2 Weather Model Runs and Data Extraction

WPS and WRF were setup to process one month per model run for the six years; 2006 to 2011. Accordingly, 72 individual WRF model runs were packaged up and run in Australia's National Computing Infrastructure. A WRF run time-step of 90 seconds was used. WRF output was segmented into daily data output files for each month of each year to simplify the variable extraction process.

WRF netCDF output files were processed with the well-known netCDF Operator (NCO) software toolkit (Zender, 2008) to extract the three required variables. WRF wind output is retained as two Cartesian coordinate parameters – U and V wind vector components. "U" wind is air motion in the "x" direction and "V" wind is air motion in the "y" direction (Stull, 2000). WRF outputs PBL height in a variable PBLH. These three variables were extracted from the daily files and averaged per month and redeposited in netCDF files retaining the model grid point latitude and longitude variables so that the files could be ingested into ArcGIS. The daily files were then used separately to output the maps of each variable for each day of 2011.

2. Monthly predictions of NO_2 concentration in South-east Queensland

The seasons in Australia are described in the following way: Spring - the three transition months September, October and November. Summer - the three hottest months December, January and February. Autumn- the transition months March, April and May (Bureau of Meteorology, 2017).

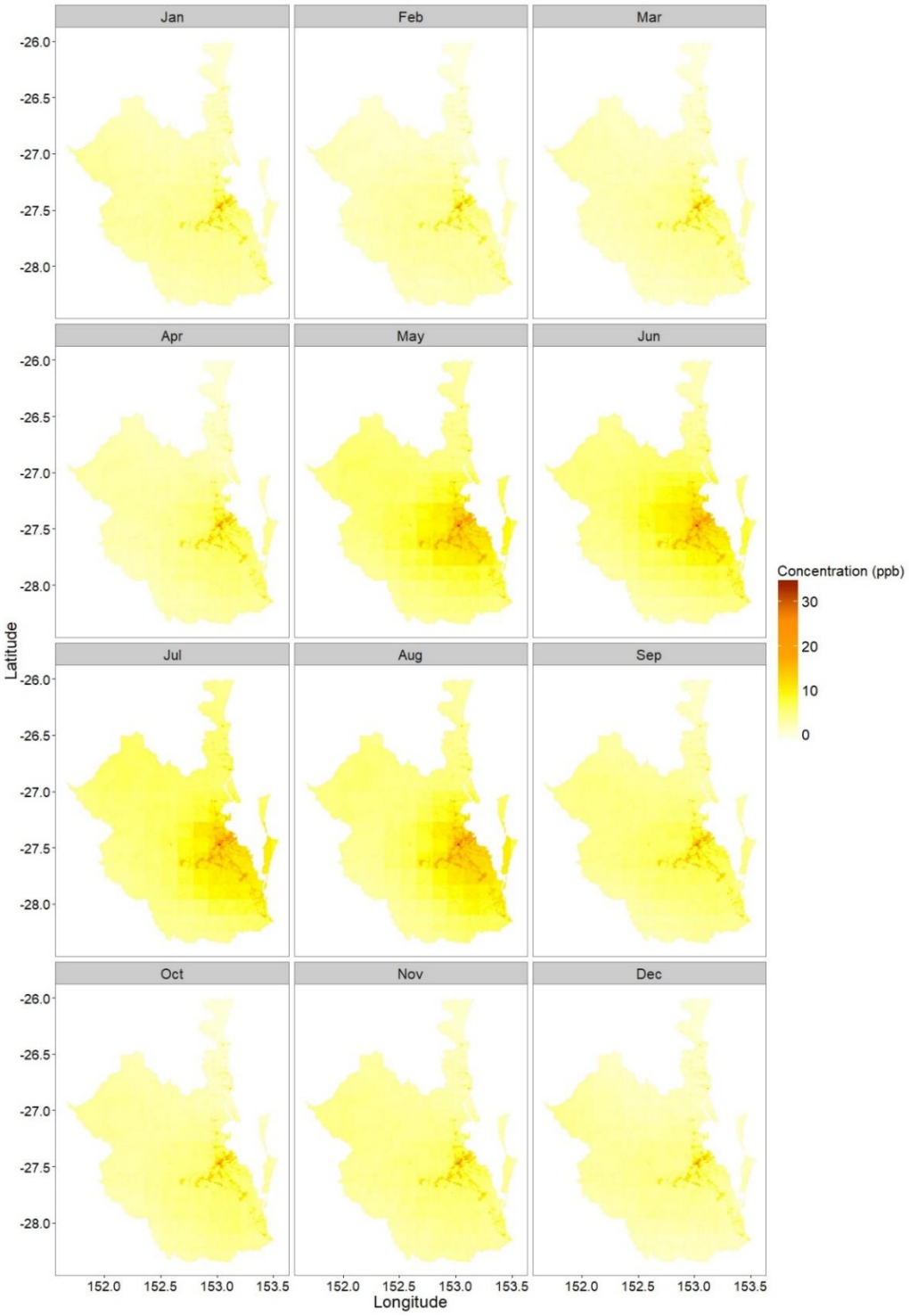

Figure S2: Monthly average predictions of NO_2 concentration in 2006.

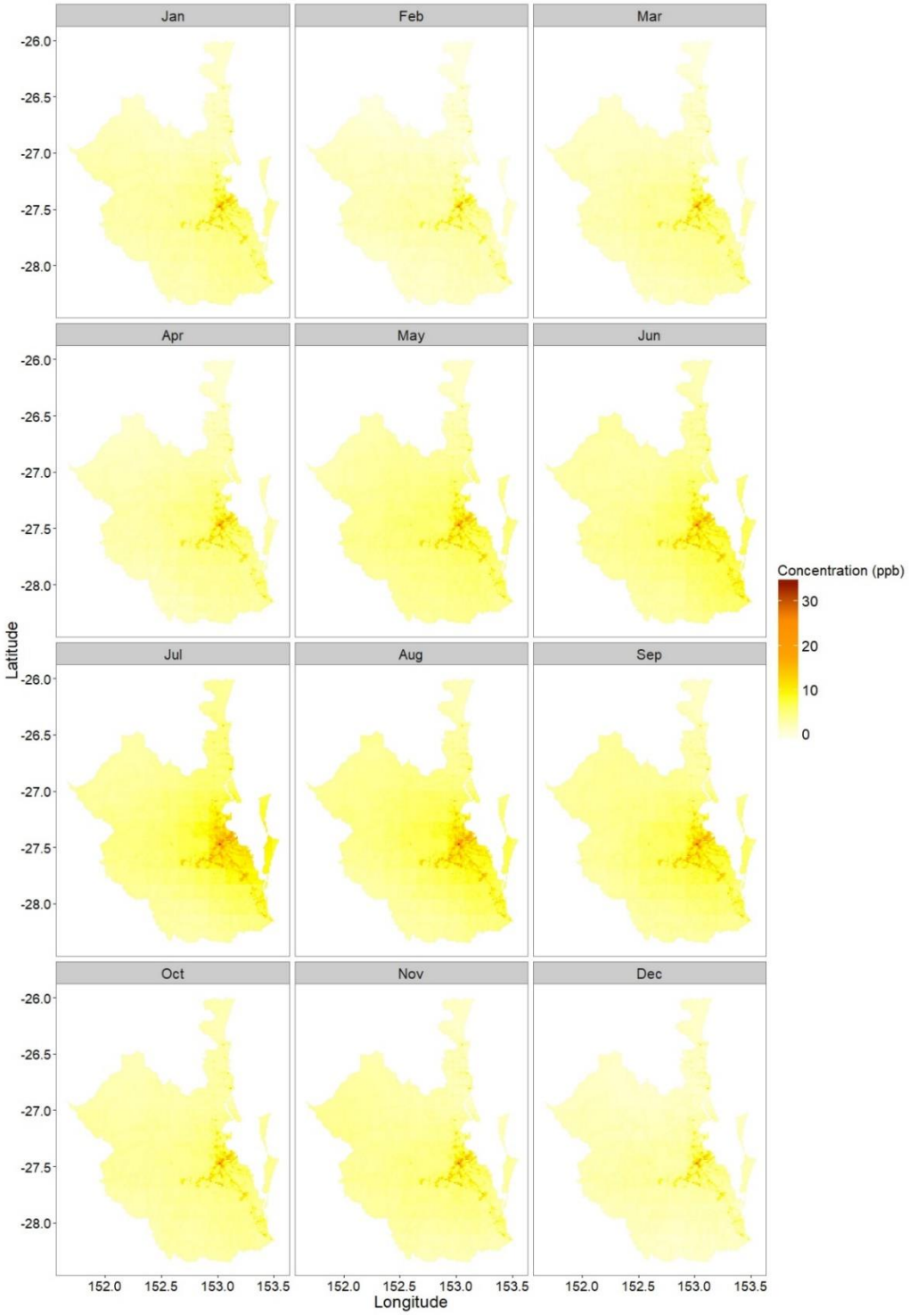

Figure S3: Monthly average predictions of NO_2 concentration in 2011.

3. Results of input selection

Table S1: Results of input selection for model A, B, C, and D.

	Std. Error	t value	Pr(>|t|)	Variance Inflation Factor
Model A				
MinorRoad_800[a]	5.77e-05	7.50	2.05e-13	1.82
Industrial_400[b]	1.90e-03	20.40	< 2e-16	1.38
MajorRoad_500[c]	1.01e-04	9.76	< 2e-16	2.01
WS[d]	6.52e-05	-9.44	< 2e-16	1.03
Model B				
ON[e]	1.75e-04	30.64	< 2e-16	1.30
MinorRoad_800	3.82e-05	11.32	< 2e-16	1.97
Industrial_400	1.24e-03	12.37	< 2e-16	1.46
MajorRoad_500	6.49e-05	18.69	< 2e-16	2.05
VI[f]	9.71e-04	-7.36	1.01e-05	1.37
WS	4.55e-05	-8.20	2.28e-05	1.23
Model C				
ON	2.06e-04	24.25	< 2e-16	1.31
TrfLen_500[g]	1.29e-09	22.07	< 2e-16	4.36
CongCount_1000[h]	6.47e-06	9.20	< 2e-16	4.46
Industrial_400	1.59e-03	8.18	< 2e-16	1.65
VI	5.11e-04	-6.41	5.23e-05	1.29
WS	5.33e-05	-7.61	4.96e-05	1.21
Model D				
ON	1.72e-04	31.07	< 2e-16	1.31
TrfLen_500	8.18e-10	18.61	< 2e-16	4.90
CongCount_1000	2.57e-05	9.20	< 2e-16	4.61
MinorRoad_800	4.01e-05	7.73	< 2e-16	2.29
Industrial_400	1.29e-03	12.37	< 2e-16	1.66
VI	9.50e-04	-6.18	3.13e-05	1.39
WS	2.55e-05	-8.21	2.72e-05	1.21

[a] The minor road variable includes sum of minor roads' length within a 800m buffer.
[b] The industrial variable includes sum of industrial land use area within a 400m buffer.
[c] The major road variable includes sum of major roads' length within a 500m buffer.
[d] Wind speed.
[e] OMI tropospheric NO_2 column density.
[f] Normalized difference vegetation index.
[g] Traffic-length interaction within a 500m buffer.
[h] The frequency of the congestion occurrence within a 1000m buffer.

4. Air quality monitoring stations

The location and the distance between the air quality monitoring (AQM) stations are shown in Figure S4 and Table S2, respectively. The spatial resolution of the satellite observations is 13 km × 24 km, while the average distance between the AQM stations in the study area is 52.23 km. Hence, the resolution of the satellite observation is finer than the spatial distribution of the AQM stations. Therefore, the use of the satellite observations provided informative data for estimating the NO_2 concentration between the stations and improved the modelling performance.

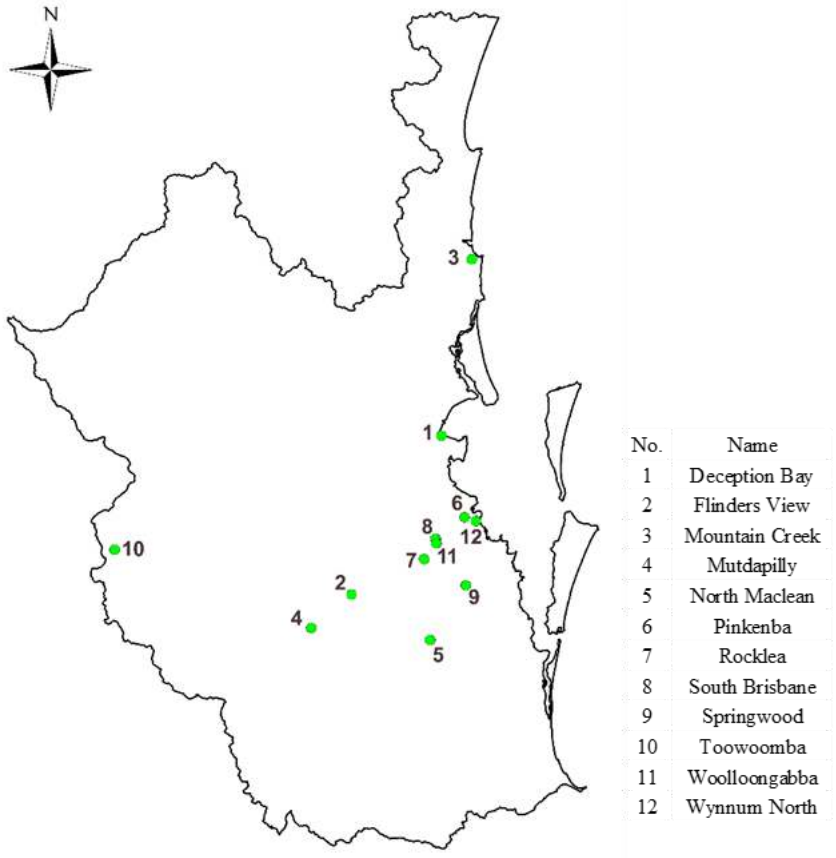

Figure S4. The location of the air quality monitoring stations in the study area

Six monitoring stations operated during the whole study period, while other stations did not measure the NO_2 concentration continuously throughout the study period. A summary of the missing data period in the monitoring stations is provided in the following:

- Pinkenba: January 2011

- Rocklea: March 2008, February 2011 to December 2011
- Springwood: February 2006
- Toowoomba: January to December 2011
- Woolloongabba: January 2006 to March 2008
- Wynnum North: January 2006 to August 2007

Table S2: The distance between air quality monitoring stations within the study area (km).

	Deception Bay	Flinders View	Mountain Creek	Mutdapilly	North Maclean	Pinkenba	Rocklea	South Brisbane	Springwood	Toowoomba	Woolloongabba	W
Deception Bay	0											
Flinders View	57.26	0										
Mountain Creek	56.19	111.88	0									
Mutdapilly	72.92	16.66	126.32	0								
North Maclean	64.22	28.53	120.35	37.49	0							
Pinkenba	26.62	43.01	81.15	59.26	39.78	0						
Rocklea	39.17	25.26	95.33	41.57	25.19	18.43	0					
South Brisbane	32.41	31.68	88.65	48.15	31.79	11.23	7.38	0				
Springwood	47.72	36.1	102.76	50.49	20.52	21.29	15.55	17.53	0			
Toowoomba	109.19	75.99	144.78	66.94	103.39	110.89	97.53	101.17	111.28	0		
Woolloongabba	33.8	31.6	89.37	47.24	30.31	12.19	6.25	1.44	16.43	101.25	0	
Wynnum North	28.99	45.49	82.25	61.76	39.94	3.84	20.18	13.92	20.44	114.37	14.32	

5. Model evaluation metrics

Different metrics can be used for evaluating the modelling performance. In this study, the coefficient of determination (R^2) was utilized to describe the proportion of the variation in the dependent variable(s) which can be explained by a model of interest (Yeganeh et al., 2012), and it is calculated as bellow:

$$R^2 = 1 - \frac{\sum_{i=1}^{n}\left(Y_i - Y_i^*\right)^2}{\sum_{i=1}^{n}(Y_i - \bar{Y}_i)^2} \quad (1)$$

In addition, the root mean squared error (RMSE) was used to evaluate the accuracy of the modelling performance using equation 2:

$$RMSE = \sqrt{\frac{1}{n}\sum_{i=1}^{n}\left|Y_i - Y_i^*\right|^2} \quad (2)$$

where i indicates the number of the samples, Y_i is the observation value, $\bar{Y}_i$ is the average of observations, and Y_i^* is the predicted value.

References

Bureau of Meteorology, 2017. Climate Glossary.

Deppe, A.J., Gallus, W.A., Takle, E.S., 2013. A WRF Ensemble for Improved Wind Speed Forecasts at Turbine Height. Weather Forecast. 28(1) 212-228.

Evans, J., Ekström, M., Ji, F., 2012. Evaluating the performance of a WRF physics ensemble over South-East Australia. Climate Dyn. 39(6) 1241-1258.

Horvath, K., Koracin, D., Vellore, R., Jiang, J., Belu, R., 2012. Sub- kilometer dynamical downscaling of near- surface winds in complex terrain using WRF and MM5 mesoscale models. Journal of Geophysical Research: Atmospheres 117(D11).

Santos-Alamillos, F.J., Pozo-Vázquez, D., Ruiz-Arias, J.A., Lara-Fanego, V., Tovar-Pescador, J., 2013. Analysis of WRF Model Wind Estimate Sensitivity to Physics Parameterization Choice and Terrain Representation in Andalusia (Southern Spain). J. Appl. Meteor. Climatol. 52(7) 1592-1609.

Skamarock, W.C., Klemp, J.B., Dudhia, J., Gill, D.O., Barker, D.M., Wang, W., Powers, J.G., 2005. A description of the advanced research WRF version 2. DTIC Document.

Stull, R.B., 2000. Meteorology for scientists and engineers: a technical companion book with Ahrens' Meteorology Today. Brooks/Cole.

Wang, W., Bruyere, C., Duda, M., Dudhia, J., Gill, D., Kavulich, M, K., K, L., H-C, Michalakes, , R., S, Zhang, X., 2012. Weather Research and Forecasting ARW Version 3 Modeling System User's Guide, : National Center for Atmospheric Research, Boulder CO USA.

Yang, Q., Berg, L.K., Pekour, M., Fast, J.D., Newsom, R.K., Stoelinga, M., Finley, C., 2013. Evaluation of WRF-Predicted Near-Hub-Height Winds and Ramp Events over a Pacific Northwest Site with Complex Terrain. J. Appl. Meteor. Climatol. 52(8) 1753-1763.

Yeganeh, B., Motlagh, M.S.P., Rashidi, Y., Kamalan, H., 2012. Prediction of CO concentrations based on a hybrid Partial Least Square and Support Vector Machine model. Atmospheric environment 55 357-365.

Zender, C.S., 2008. Analysis of self-describing gridded geoscience data with netCDF Operators (NCO). Environmental Modelling & Software 23(10–11) 1338-1342.

Zhang, H., Pu, Z., Zhang, X., 2013. Examination of Errors in Near-Surface Temperature and Wind from WRF Numerical Simulations in Regions of Complex Terrain. Weather Forecast. 28(3) 893-914.